J Solution Chem (2007) 36: 723–765
DOI 10.1007/s10953-007-9145-2

ORIGINAL PAPER

Phase Behavior of Aqueous Na–K–Mg–Ca–Cl–NO_3 Mixtures: Isopiestic Measurements and Thermodynamic Modeling

Mirosław S. Gruszkiewicz · Donald A. Palmer · Ronald D. Springer · Peiming Wang · Andrzej Anderko

Received: 12 October 2006 / Accepted: 28 November 2006 /
Published online: 11 May 2007

Abstract A comprehensive model has been established for calculating thermodynamic properties of multicomponent aqueous systems containing the Na^+, K^+, Mg^{2+}, Ca^{2+}, Cl^- and NO_3^- ions. The thermodynamic framework is based on a previously developed model for mixed-solvent electrolyte solutions. The framework has been designed to reproduce the properties of salt solutions at temperatures ranging from the freezing point to 300 °C and concentrations ranging from infinite dilution to the fused salt limit. The model has been parameterized using a combination of an extensive literature database and new isopiestic measurements for thirteen salt mixtures at 140 °C. The measurements have been performed using Oak Ridge National Laboratory's (ORNL) previously designed gravimetric isopiestic apparatus, which can also detect solid phase precipitation. In addition to various Na–K–Mg–Ca–Cl–NO_3 systems, results are reported for LiCl solutions. Water activities are reported for mixtures with a fixed ratio of salts as a function of the total apparent salt mole fraction. The isopiestic measurements reported here simultaneously reflect two fundamental properties of the system, i.e., the activity of water as a function of solution concentration and the occurrence of solid–liquid transitions. The thermodynamic model accurately reproduces the new isopiestic data as well as literature data for binary, ternary and higher-order subsystems. Because of its high accuracy in calculating vapor–liquid and solid–liquid equilibria, the model is suitable for studying deliquescence behavior of multicomponent salt systems.

Keywords Osmotic coefficient · Activity coefficient · Isopiestic measurements · Thermodynamic model · Deliquescence · Fused salt · Mixed brines

M.S. Gruszkiewicz · D.A. Palmer
Chem. Sciences Division, Oak Ridge National Laboratory, PO Box 2008, MS 6110, Oak Ridge, TN 37831-6110, USA

R.D. Springer · P. Wang · A. Anderko (✉)
OLI Systems Inc., 108 American Road, Morris Plains, NJ 07950, USA
e-mail: aanderko@olisystems.com

1 Introduction

Accurate knowledge of the deliquescence behavior of multicomponent brines is expected to enhance the understanding of the evolution of the chemical environment in contact with metal surfaces at the proposed radioactive waste repository at Yucca Mountain, Nevada, USA. It is anticipated that a layer of dust containing volcanic tuff and a mixture of salts originating from evaporation of seepage waters will tend to accumulate over time on all surfaces. The air inside the placement drifts will be relatively dry after final closure due to the temperature remaining well above the boiling point of water. As the temperature slowly decreases for several centuries due to radioactive decay, the relative humidity may reach sufficiently high levels for the mixture of initially dry salts to form concentrated brines through deliquescence. The concentrations of ions present in solutions contacting metal surfaces affect corrosion processes as, for example, the Cl^-/NO_3^- ratio is an important consideration in corrosion calculations. Hence, thermodynamic properties of mixed aqueous solutions are needed for reliable predictions of the composition of the brines formed under the expected scenarios of in-drift temperature and humidity evolution.

Complete phase diagrams, showing relative humidity (or water activity) as a function of composition, are scarce even for solutions containing two salts. There are very few accurate experimental data sets available on deliquescence behavior of multicomponent aqueous salt solutions at elevated temperatures. This underscores the importance of having an accurate thermodynamic model that would be capable of predicting the behavior of multicomponent systems in a wide temperature range using parameters determined from limited experimental data. While the well-known Pitzer ion-interaction model provides a useful framework for the prediction of solubilities in multicomponent solutions using activity data on binary systems with a common ion, the temperature dependence of solute-specific parameters is often not available with sufficient accuracy. Also, the molality-based Pitzer model is applicable for concentrations typically up to ca. 6 $mol \cdot kg^{-1}$, which is often insufficient for highly concentrated systems that contain nitrates. Thus, it is necessary to develop a model that would be applicable to multicomponent, concentrated solutions up to solid saturation or, under some conditions, even the fused salt limit. Further, it is desirable to verify model results against measurements made in the temperature range that is of direct interest for studying deliquescence phenomena.

The main purpose of the measurements described here is to demonstrate that the unique ORNL high-temperature isopiestic apparatus can be used to investigate the relationship between deliquescence, relative humidity (*RH*) and temperature for multicomponent aqueous solutions. The points where a new phase appears or disappears can be detected when a series of measurements of solvent mass and the corresponding vapor pressure are made as water is added or withdrawn. When the relative humidity over a mixture of solid salts increases, the solution first appears at the eutonic point of the mixture where the solution is simultaneously saturated with respect to all components. The relative humidity at the eutonic point, the mixture deliquescence *RH*, is the lowest relative humidity coexisting with a liquid solution. The tendency to deliquesce (the hygroscopic character) of solutes depends mainly on their solubility, but also on the particular character of solute-solvent interactions, described also as nonideality, or vapor-pressure lowering ability. Because an addition of a new electrolyte to a saturated solution initially lowers its vapor pressure without causing precipitation, the deliquescence *RH* of multicomponent solutions decreases as the number of solutes increases.

The second objective of this paper is to develop a comprehensive thermodynamic model for predicting the thermodynamic behavior of aqueous mixtures containing the Na^+, K^+,

Ca^{2+}, Mg^{2+}, Cl^- and NO_3^- ions. These are the key ionic components in natural environments that may give rise to the formation of concentrated solutions through deliquescence phenomena. Comprehensive modeling of such mixtures requires calibrating the model to match the properties of the constituent binary (i.e., salt–water), ternary (i.e., salt 1–salt 2–water) and higher-order subsystems. For all such systems, the primary requirement for the model is to reproduce the solid–liquid equilibria and vapor pressures as a function of temperature and composition. In the development of the model, both literature data and the new isopiestic measurements are used. Whereas literature data are primarily used to ensure the correct representation of the properties of simpler (i.e., binary and ternary) subsystems, the new isopiestic data are essential for verifying the performance of the model for concentrated multicomponent mixtures at high temperatures.

2 Experimental

The isopiestic method is based on equilibration of a number of solutions together with reference standards in a common chamber, until all transfer of the solvent ceases and all solutions reach the same water activity. The ORNL high-temperature isopiestic apparatus, described previously [1–5], has been used during the last several decades to measure vapor pressures and obtain osmotic and activity coefficients for many aqueous solutions of pure electrolytes and their mixtures at temperatures typically between 110 and 250 °C. The main feature of this apparatus is its internal electromagnetic balance with optical detection. Since only the solvent is exchanged between samples while the masses of nonvolatile solutes placed initially in the platinum cups remain constant, the amounts of water present at any time and hence the molalities of the solutions can be determined gravimetrically without interrupting the equilibrium. The isopiestic apparatus provides, in general, a greater reliability and accuracy of the results than other recently reported experimental methods of investigating deliquescence [6, 7] thanks to the precise control of relative humidity over arbitrarily long times, the absence of atmospheric air, the high accuracy of the gravimetric method for molality and of the relative isopiestic method for vapor pressure, and the fast equilibration times due to the efficient heat exchange between the solution cups.

The internal balance was calibrated during each series of weighings using platinum and titanium mass standards placed in the sample holder between the sample cups. All twenty cups containing the samples, the reference solutions and the mass standards were weighed at each equilibrium point two to three times. The corrections for buoyancy in water or air were applied to all weighings. Each solution contained 10 to 15 mmole of salts (about 1 g) and no more than 3 g of water. The accuracy of the balance was better than ±1 mg. The estimated absolute error of the resulting average molalities m ($mol \cdot kg^{-1}$) was less than 0.0001 $mol \cdot kg^{-1}$.

The apparatus was also equipped with quartz pressure transducers (Digiquartz, Paroscientific, Inc.) allowing for accurate monitoring of the approach to equilibrium. The set of four Digiquartz transducers (with the ranges of 2.1, 6.9, 21 and 69 bar), kept in an air oven at a constant temperature of about 39.0 ± 0.1 °C, provided an accurate and relatively simple means of measuring water vapor pressure. Although only a dead-weight instrument with a precise pressure difference indicator could deliver a substantially greater accuracy, at 140 °C, and at the pressures between 0.35 bar and 2.7 bar, the relative isopiestic method based on reference solutions was still significantly superior to direct pressure measurement. The accuracy of the direct pressure measurement was limited by the effects of temperature, viscosity, surface tension and hydrostatic pressure of the liquid water present inside

the transducers and in the tubing connecting them to the vapor space maintained at elevated temperature. The results reported here are not based on the measured pressures, but instead on the calcium chloride reference solution [5].

Stock solutions were prepared by weight using distilled and deionized water (from a Barnstead NANOpure four-stage water purification system) and the chemicals supplied by Alfa Aesar Chemical Co. without any purification other than drying. Two grades of pure salts were used. The chlorides were the "ultra dry" grade chemicals with metal-basis purities specified by the vendor as 0.99998 for NaCl and KCl, 0.99995 for LiCl, and 0.9999 for $CaCl_2$ and $MgCl_2$. These salts, received in the form of powders or small beads stored in glass ampoules under argon, were also certified to contain at most 100 ppm oxide and hydroxide, and were used without drying. The nitrates of sodium, potassium, calcium and magnesium were "Puratronic" grade chemicals with metal-basis purities better than 0.99995. These salts, in particular the hydrates of $Ca(NO_3)_2$ and $Mg(NO_3)_2$, were dried carefully in a vacuum oven for several days, while avoiding deliquescence and possible decomposition by slowly increasing temperature to about 140 °C.

All stock solutions of the "ultra dry" salts contained some amount of insoluble impurities. In the case of $CaCl_2$ and $MgCl_2$ this was determined by XRD to be mostly sulfate. The exact quantities of impurities were not determined; however, they were apparently higher than expected for these types of chemicals. It is likely that the purity of these materials was lower than stated by the vendor. There were no noticeable insoluble impurities in the solutions of the "Puratronic" salts.

This work describes the first use of the ORNL isopiestic apparatus specifically for determination of solubilities in multi-component solutions. The water initially injected into the apparatus was previously degassed by boiling and sparging with helium. The solutions were all liquid at the starting relative humidity of 75%. The relative humidity was then decreased in about 20 steps to the final value of 10% by releasing water from the autoclave under atmospheric pressure or vacuum when necessary. At least 16 hours were allowed for equilibration at each step. Since the measurements started with liquid samples of approximately the same molality as the stock solutions, it was convenient to conduct the measurements by progressively decreasing the relative humidity. The process observed was in fact precipitation (efflorescence) of salts from the solution instead of deliquescence. However, measurements can be also be made in the reverse direction by starting from solid salt mixtures. It is assumed that the results are completely reversible with respect to the direction of the changes in relative humidity.

The phase changes occurring in the mixed solutions were clearly visible as breaks in the curve representing initially the osmotic coefficient of the solution as a function of relative humidity. The osmotic coefficient, ϕ, was calculated as

$$\phi = 1000 w_s / M_s \sum n_i \ln a_s \tag{1}$$

where M_s (g·mol^{-1}) is the molecular weight of water, a_s is the activity of water, n_i are the numbers of moles for each ion and w_s (kg) is the mass of water. The value of a_s is obtained from values calculated for an aqueous reference $CaCl_2$ solution. Naturally, after the appearance of a solid phase, because the distribution of the salts between solid and liquid phases is not known, the quantity calculated from the above equation does not represent the actual osmotic coefficient. As the first component begins to precipitate from the solution, the ratio n_i/w_s exceeds the actual molality of the liquid phase and the osmotic coefficient appears to decrease sharply. This process continues gradually as the relative humidity continues to

Table 1 Compositions of the samples. Solute contents in each cup are given as the total number of millimoles corresponding to the salt formula

1.	NaCl: 14.672
2.	$NaCl + NaNO_3$: 7.4646 + 6.8248
3.	$Mg(NO_3)_2$: 8.8921
4.	$NaNO_3 + KNO_3 + Ca(NO_3)_2 + Mg(NO_3)_2$: 5.2873 + 1.2967 + 2.3614 + 1.2197
5.	$CaCl_2 + MgCl_2 + Ca(NO_3)_2 + Mg(NO_3)_2$: 5.0878 + 0.77353 + 2.6309 + 1.4123
6.	LiCl: 13.197
7.	$NaCl + KCl + NaNO_3 + KNO_3$: 5.4795 + 2.3108 + 2.7690 + 1.0563
8.	$KCl + KNO_3$: 8.1026 + 2.8021
9.	$NaCl + KCl + NaNO_3 + KNO_3 + CaCl_2 + MgCl_2 + Ca(NO_3)_2 + Mg(NO_3)_2$: 4.1946 + 2.0027 + 2.8693 + 0.70451 + 0.53286 + 0.20404 + 0.40974 + 0.13368
10.	$NaNO_3 + KNO_3$: 9.0689 + 2.2832
11.	$CaCl_2$: 9.3057
12.	$Ca(NO_3)_2$: 7.9988
13.	$CaCl_2 + Ca(NO_3)_2$: 4.5080 + 4.0814

decrease and more water evaporates from the solution. After reaching the eutonic composition, all the remaining water evaporates at a constant relative humidity. By using samples of varying solute ratios, a complete solubility diagram can be obtained.

The compositions of the samples are summarized in Table 1. For each of the 13 samples defined in Table 1, Table 2 gives the masses of water (and, hence, the overall system compositions) that correspond to 21 values of the water activity. Note that in one case (sample cup 8 containing $KCl + KNO_3$) a deficit of mass has been found. The negative values assigned to water mass in Table 1, amounting to nearly 3% of the initial amount of water, reflect in fact the difference between the final and the initial masses of the salts. The source of this error was not determined with certainty; it could be due to either a loss of stock solution when initially injecting the samples, or, more likely, a splatter of a drop of the solution during stepwise water removal from the autoclave. To avoid violent boiling, the pressure has to be reduced very slowly, in particular when the solutions are close to saturation. However, the extremely slow rates of water removal required to guarantee no splatter were impractical, and occasional violent releases of steam bubbles could not be ruled out. Using taller sample cups with lids made of platinum mesh could reduce the likelihood of a drop of solution leaving a sample cup.

3 Thermodynamic Model

For modeling the properties of aqueous Na–K–Ca–Mg–Cl–NO_3 mixtures, we use a thermodynamic framework that has been previously developed at OLI Systems for mixed-solvent electrolyte systems (Wang et al. [8–10]). This framework is capable of reproducing the properties of multicomponent salt solutions ranging from infinite dilution to the fused salt limit and, therefore, it is particularly suitable for studying deliquescence phenomena. The model was described in detail in previous papers [8–10] and, therefore, only a brief summary is given here.

The thermodynamic framework combines an excess Gibbs energy model for mixed-solvent electrolyte systems with a comprehensive treatment of chemical equilibria. In this

Table 2 Masses of water (mg) in each of the 13 sample cups at 21 values of water activity a ($t = 140$ °C)

a	1	2	3	4	5	6	7	8	9	10	11	12	13
0.7507	2172.1	1863.4	2651.5	1478.9	2557.9	2367.1	1491.8	1204.5	1560.0	1141.8	2582.4	1640.3	2077.1
0.7270	12.5	1683.9	2476.5	1343.0	2376.2	2200.8	1348.8	1079.7	1414.0	1016.1	2409.4	1513.0	1925.0
0.6852	3.3	1425.4	2218.2	1149.2	2111.5	1962.1	1143.1	907.3	1207.5	834.0	2149.1	1321.7	1699.2
0.6529	3.3	1030.9	2051.2	1028.7	1936.0	1804.0	902.9	429.2	1070.2	724.5	1975.8	1199.3	1549.6
0.6333	5.5	825.7	1961.8	963.4	1844.2	1723.1	690.1	298.3	944.5	666.9	1879.7	1136.7	1474.8
0.6198	4.2	716.5	1899.6	921.1	1781.7	1667.0	578.0	241.1	799.1	631.9	1816.9	1095.3	1422.4
0.6099	6.0	649.9	1863.1	894.6	1739.6	1626.5	511.2	208.1	715.5	609.0	1772.4	1067.8	1385.8
0.5984	5.1	593.4	1814.7	864.5	1693.2	1582.3	452.8	183.1	650.2	579.7	1722.5	1035.6	1347.0
0.5769	6.7	510.5	1738.5	813.0	1612.6	1510.1	369.3	139.1	543.3	532.6	1633.7	982.9	1277.5
0.5765	4.2	505.3	1730.6	806.2	1608.2	1507.1	365.9	137.6	540.3	533.3	1632.0	975.8	1274.4
0.5507	6.5	431.2	1645.0	749.1	1518.2	1421.9	287.9	102.4	447.4	482.9	1532.7	917.1	1197.7
0.5168	4.6	356.6	1541.2	680.0	1408.6	1325.6	222.2	73.5	362.9	424.6	1412.0	845.1	1106.3
0.4979	3.8	324.1	1490.3	646.7	1356.1	1273.5	192.4	59.5	326.8	395.8	1349.3	809.7	1060.2
0.4423	1.9	250.1	1350.4	556.9	1206.7	1133.7	131.5	31.7	246.6	324.1	1180.0	711.1	934.6
0.3858	5.5	9.3	1224.3	479.8	1074.7	1005.2	92.4	−31.1	192.7	261.4	1026.2	623.9	823.8
0.3451	4.6	8.3	1140.1	429.6	986.9	917.9	73.2	−32.9	163.7	128.1	923.8	565.0	748.8
0.3000	7.0	9.7	1045.4	374.7	889.7	821.6	54.4	−30.1	137.4	87.1	817.8	498.3	664.3
0.2424	7.5	10.0	931.4	306.1	772.7	700.8	9.9	−32.2	108.1	46.8	693.4	423.6	569.0
0.2080	5.5	9.4	865.6	263.7	707.1	628.0	4.2	−32.2	92.4	2.2	625.3	376.9	513.9
0.1486	5.1	7.0	751.5	202.9	597.9	513.4	3.4	−30.4	69.3	1.5	516.2	94.4	418.4
0.1023	8.4	9.4	609.1	147.8	474.0	6.0	4.9	−32.3	44.7	2.3	398.3	4.3	306.2

framework, the excess Gibbs energy is expressed as

$$\frac{G^{ex}}{RT} = \frac{G^{ex}_{LR}}{RT} + \frac{G^{ex}_{II}}{RT} + \frac{G^{ex}_{SR}}{RT} \tag{2}$$

where G^{ex}_{LR} represents the contribution of long-range electrostatic interactions, G^{ex}_{II} accounts for specific ionic (ion–ion and ion–molecule) interactions and G^{ex}_{SR} is the short-range contribution resulting from intermolecular interactions.

The long-range interaction contribution is calculated from the Pitzer–Debye–Hückel formula [11] expressed in terms of mole fractions and symmetrically normalized, i.e.,

$$\frac{G^{ex}_{DH}}{RT} = -\left(\sum_i n_i\right)\frac{4A_x I_x}{\rho}\ln\left(\frac{1+\rho I_x^{1/2}}{\sum_i x_i[1+\rho(I^0_{x,i})^{1/2}]}\right) \tag{3}$$

where the sum is over all species, I_x is the mole fraction-based ionic strength, $I^0_{x,i}$ represents the ionic strength when the system composition reduces to a pure component i, i.e., $I^0_{x,i} = 0.5z_i^2$; ρ is related to the hard-core collision diameter ($\rho = 14.0$) and the A_x parameter is given by

$$A_x = \frac{1}{3}(2\pi N_A d_s)^{1/2}\left(\frac{e^2}{4\pi\varepsilon_0\varepsilon_s k_B T}\right)^{3/2} \tag{4}$$

where d_s and ε_s are the molar density and dielectric constant of the solvent, respectively. The specific ion-interaction contribution is calculated from an ionic strength-dependent, symmetrical second virial coefficient-type expression [8]:

$$\frac{G^{ex}_{II}}{RT} = -\left(\sum_i n_i\right)\sum_i\sum_j x_i x_j B_{ij}(I_x) \tag{5}$$

where $B_{ij}(I_x) = B_{ji}(I_x)$, $B_{ii} = B_{jj} = 0$ and the ionic strength dependence of B_{ij} is given by

$$B_{ij}(I_x) = b_{ij} + c_{ij}\exp(-\sqrt{I_x + a_1}) \tag{6}$$

and where b_{ij} and c_{ij} are binary interaction parameters and a_1 is set equal to 0.01. In general, the parameters b_{ij} and c_{ij} are represented as functions of temperature as

$$b_{ij} = b_{0,ij} + b_{1,ij}T + b_{2,ij}/T + b_{3,ij}T^2 + b_{4,ij}\ln T \tag{7}$$

$$c_{ij} = c_{0,ij} + c_{1,ij}T + c_{2,ij}/T + c_{3,ij}T^2 + c_{4,ij}\ln T. \tag{8}$$

The last two parameters of Eqs. 7 and 8 are typically necessary only when there is a need to reproduce experimental data over a very wide range of temperatures, e.g., from −50 to 300 °C. Finally, the short-range interaction contribution is calculated from the UNIQUAC equation [12]. In systems containing only strong electrolytes, such as the Na–K–Ca–Mg–Cl–NO_3 mixtures considered here, the short-range term is unnecessary and all interactions are accounted for by Eq. 5.

The excess Gibbs energy model is used to calculate nonideality effects on solid–liquid equilibria and chemical equilibria, such as ion pairing. For example, solubility of a salt MX is represented as a chemical equilibrium between the solid salt MX(s) and the ions that result from its dissociation, M^{m+} and X^{x-}. The chemical equilibrium is governed by the chemical

potentials of all species that participate in a given reaction. The chemical potential of each ionic or neutral species i is determined by its standard-state contribution, $\mu_i^{\mathrm{o}}(T, P)$, and its activity coefficient, $\gamma_i(T, p, \boldsymbol{x})$, i.e.,

$$\mu_i(T, p, x) = \mu_i^{\mathrm{o}}(T, p) + RT \ln x_i \gamma_i(T, p, x). \tag{9}$$

The standard-state chemical potentials for aqueous species, $\mu_i^{\mathrm{o}}(T, p)$, are calculated as functions of temperature and pressure using the Helgeson–Kirkham–Flowers–Tanger (HKF) equation of state [13, 14]. The parameters of the HKF model are available for a large number of aqueous species including ions and ion pairs [15, 18]. It should be noted that standard-state properties calculated from the model of Helgeson et al. are based on the infinite-dilution reference state and on the molality concentration scale. To make the equilibrium calculations consistent when the standard-state properties are combined with the mole fraction-based and symmetrically normalized activity coefficients, two conversions are performed: (1) the activity coefficients calculated from Eq. 2 are converted to those based on the unsymmetrical reference state, i.e., at infinite dilution in water, and (2) the molality-based standard-state chemical potentials are converted to corresponding mole fraction-based quantities [8].

4 Determination of Parameters

The parameters of the model are determined using thermodynamic data of various types, including

(1) vapor–liquid equilibria
(2) activity and osmotic coefficients
(3) solid–liquid equilibria
(4) enthalpies of dilution or mixing
(5) heat capacities
(6) densities.

The parameters for the Na–K–Mg–Ca–Cl–NO_3 systems were evaluated and/or verified using a combination of literature data and the new isopiestic data reported in this study. There is a very large body of literature data that covers all the eight binary subsystems (i.e., NaCl, KCl, $MgCl_2$, $CaCl_2$, $NaNO_3$, KNO_3, $Mg(NO_3)_2$ and $Ca(NO_3)_2$ with H_2O), most of the twenty-eight possible ternary subsystems and an appreciable number of quaternary and quinary subsystems of this ternary mixture [7, 19–304]. References to binary and ternary data are collected in Table 3 in the form of a matrix defined by the eight fundamental constituent salts. The diagonal elements of the matrix (i.e., salt A–salt A) show references to the sources of experimental data for the binary subsystems (i.e., salt A–H_2O). The off-diagonal elements refer to the data for the ternary subsystems (i.e., salt A–salt B–H_2O). As shown in Table 3, there is a wealth of information for all binary systems. In the case of the ternary subsystems, there is extensive experimental coverage for mixtures containing two chlorides. Also, there are a reasonable number of experimental data sources for the ternaries that contain two nitrates and those that combine the nitrates and chlorides of sodium and potassium. However, the experimental coverage is much sparser for mixed chloride–nitrate ternaries that contain magnesium and calcium in addition to sodium and potassium.

Table 4 summarizes the sources of experimental data for quaternary and higher-order systems. Since a complete matrix representation is not practical in this case, Table 4 groups the subsystems according to the availability of experimental data. It is noteworthy that a fairly

Table 3 Summary of references to experimental data sources for binary and ternary aqueous solutions containing Na, K, Mg, Ca, Cl and NO_3 salts

	NaCl	KCl	$MgCl_2$	$CaCl_2$	$NaNO_3$	KNO_3	$Mg(NO_3)_2$	$Ca(NO_3)_2$
NaCl	[19–25], this work							
KCl	[165–179]	[19–21, 26–35]						
$MgCl_2$	[44–47, 165, 166, 180–203]	[48, 49, 165, 180–182, 204, 217–230]	[19, 26–28, 36–96]					
$CaCl_2$	[98, 165–169, 204–216]	[167, 204, 205, 217, 218, 231–237]	[37, 50, 51, 183, 204, 217–220, 231, 238–245]	[5, 26–28, 36–39, 97–111], this work				
$NaNO_3$	[7, 113, 123, 246–249, 272–280], this work	[113, 299]			[20, 22, 23, 26, 40–42, 112–140]			
KNO_3	[22, 23, 113, 144, 233, 246, 247, 281, 299–303]	[113, 143, 170, 232, 246–249, 272, 281–288], this work	[304]	[232]	[7, 22, 23, 113, 114, 246–257], this work	[19, 20, 22, 23, 26, 40, 41, 112–121, 141–150]		
$Mg(NO_3)_2$			[184]		[184, 258–263]	[266]	[19, 26, 27, 36, 40, 41, 43, 112, 141, 151–160], this work	
$Ca(NO_3)_2$	[22, 233]	[232, 267]		[232, 287], this work	[122, 206, 264, 265]	[232, 264, 267–269]	[270, 271]	[22, 26, 36, 40, 97, 142, 161–164]

large number of data sources deal with chloride-only multicomponent mixtures. Much less information is available for mixtures of chlorides and nitrates. Here, the new isopiestic measurements fill important gaps.

The model parameterization procedure adopted in this work consisted of several steps. First, binary parameters were determined using data for the eight binary subsystems. These

Table 4 Summary of references to experimental data for quaternary, quinary and higher-order aqueous systems containing Na, K, Mg, Ca, Cl and NO_3 salts

Salts	References
$NaCl–KCl–MgCl_2$	[52, 180, 181, 185, 186, 221, 222, 238, 290–294]
$NaCl–KCl–CaCl_2$	[166, 168, 185, 187, 207, 295]
$NaCl–MgCl_2–CaCl_2$	[183, 185, 238, 239, 296]
$KCl–MgCl_2–CaCl_2$	[219, 220, 238, 297, 298]
$NaCl–KCl–MgCl_2–CaCl_2$	[185, 238, 290, 296]
$NaCl–KCl–NaNO_3$	[246, 299]
$NaCl–KCl–KNO_3$	[246, 299]
$NaCl–NaNO_3–KNO_3$	[22, 23, 246, 250, 273, 299], this work
$KCl–NaNO_3–KNO_3$	[246, 300]
$KCl–CaCl_2–KNO_3$	[232, 267, 282]
$KCl–CaCl_2–Ca(NO_3)_2$	[232]
$CaCl_2–KNO_3–Ca(NO_3)_2$	[232, 267, 282]
$KCl–MgCl_2–Mg(NO_3)_2$	[304]
$MgCl_2–CaCl_2–Mg(NO_3)_2–Ca(NO_3)_2$	this work
$NaNO_3–KNO_3–Mg(NO_3)_2–Ca(NO_3)_2$	this work
$NaCl–KCl–MgCl_2–CaCl_2–NaNO_3–KNO_3–Mg(NO_3)_2–Ca(NO_3)_2$	this work

regressions were based on data of various types as described above. This produced the interaction parameters, Eqs. 7 and 8, between the cations and anions that constitute each subsystem. Also, thermochemical parameters (i.e., the Gibbs energy and entropy) for some hydrated salts were simultaneously adjusted to match solid–liquid equilibrium data. Such adjustments were not necessary for the solids for which thermochemical properties are known with high accuracy.

In the second step, data for ternary subsystems were used to determine the cation–cation and anion–anion interaction parameters. At the same stage, thermochemical parameters were adjusted for the double salts that do not occur in binary subsystems but precipitate in ternary and higher-order mixtures. The thermochemical properties of such double salts are typically known with lower accuracy than those of pure solids and, therefore, they needed to be adjusted to match their solubilities. Finally, data for quaternary and higher-order systems were used to verify the predictions of the model. In some cases, quaternary data were used to fine-tune model parameters when they extended to temperatures that were not covered by the relevant ternary subsystems.

In all cases, parameters were determined to cover the temperature range from the freezing point of salt solutions (typically between −50 and 0 °C) and 300 °C. The upper limit of 300 °C is an inherent limitation of excess Gibbs energy models when applied to aqueous systems. Above 300 °C, the system becomes too close to the critical locus to be handled by classical excess Gibbs energy models. However, the temperature range from the freezing point to 300 °C comfortably encompasses the conditions that are of interest for studying deliquescence.

The model parameters are summarized in Tables 5–7. Table 5 shows the standard-state properties and parameters of the HKF equation of state [13–18] for all ions and neutral aqueous species that were included in the model. All parameters for the base ions were

Table 5 Parameters used in the model for individual ionic and neutral species: standard partial molar Gibbs energy of formation, entropy, and parameters of the Helgeson–Kirkham–Flowers [13–18] equation of state for standard partial molar thermodynamic properties ($a_{HKF,1...4}$, $c_{HKF,1}$, $c_{HKF,2}$, ω)

Species	$\Delta\overline{G}_f^{o}$ kJ·mol^{-1}	$\overline{S}^{o}$ J·mol^{-1}·K^{-1}	$a_{HKF,1}$	$a_{HKF,2}$	$a_{HKF,2}$	$a_{HKF,3}$	$c_{HKF,1}$	$c_{HKF,2}$	ω
Cl^- [a]	−131.290	56.735	0.4032	480.1	5.563	−28470	−4.4	−57140	145600
NO_3^- [a]	−110.905	146.942	0.73161	678.24	−4.6838	−30594	7.7	−67250	109770
Li^+ [a]	−292.600	11.2968	−0.00237	−6.9	11.58	−27761	19.2	−2400	48620
Na^+ [a]	−261.881	58.4086	0.1839	−228.5	3.256	−27260	18.18	−29810	33060
K^+ [a]	−282.462	101.044	0.3559	−147.3	5.435	−27120	7.4	−17910	19270
Mg^{2+} [a]	−453.960	−138.100	−0.08217	−859.9	8.39	−23900	20.8	−58920	153720
Ca^{2+} [a]	−552.790	−56.484	−0.01947	−725.2	5.2966	−24792	9	−25220	123660
LiCl(aq) [b]	−391.239	112.4191	0.55837	585.54	3.4416	−30210	17.7136	11006	−3800
$MgCl_2$(aq) [b]	−623.223	2.8920	0.62187	740.58	2.8322	−30851	23.961	32720	−3800
$CaCl_2$(aq) [b]	−794.040	67.7344	0.62187	740.58	2.8322	−30851	23.961	32720	−3800

[a] All parameters were obtained from Refs. [16, 17]

[b] Standard-state properties of the ion pairs were adjusted in this study based on multiproperty regressions for binary salt–water systems

Table 6 Binary parameters used in the ionic interaction term of Eqs. 6, 7

Species i	Species j	$b_{0,ij}$	$b_{1,ij}$	$b_{2,ij}$	$b_{3,ij}$	$b_{4,ij}$	$c_{0,ij}$	$c_{1,ij}$	$c_{2,ij}$	$c_{3,ij}$	$c_{4,ij}$
NO_3^-	Na^+	252.54	−0.46165	−42982	0.00023981	0	−383.93	0.60763	70566	−0.00019394	0
NO_3^-	K^+	307.869	−0.55685	−53814	0.00030259	0	−384.39	0.55306	78130	−0.00015254	0
NO_3^-	Mg^{2+}	−151.73	0.22098	9173.9	0	0	147.37	−0.20379	−3281.9	0	0
NO_3^-	Ca^{2+}	44.229	−0.043742	−15419	0	0	−198.68	0.26781	46616	0	0
Cl^-	Li^+	75.065	−0.036110	−32492	-5.3869×10^{-5}	0	−87.198	−0.033825	43812	0.00023238	0
Cl^-	Na^+	15611	7.9642	−357990	−0.0036431	−2892.7	−30086	−15.010	699850	0.0068210	5552.3
Cl^-	K^+	15088	7.2361	−354190	−0.0031415	−2771.6	−26853	−12.857	635046	0.0056499	4927.6
Cl^-	Mg^{2+}	−46.090	0.036682	−12896	8.2938×10^{-6}	0	110.43	−0.24025	11645	0.00031976	0
Cl^-	Ca^{2+}	−95.993	0.47023	−17371	-5.6755×10^{-4}	0	−0.69437	−0.42158	43726	0.00079111	0
Cl^-	NO_3^-	15.1696	0	−5055.81	0	0	−21.0094	0	7500.53	0	0
Na^+	K^+	−93.0411	−0.234488	37002.7	5.62879×10^{-4}	0	−64.633	0.881525	−29428.5	−0.0012859	0
Na^+	Mg^{2+}	−28.8624	0.0351923	8744.27	0	0	0	0	−6373.88	0	0
Na^+	Ca^{2+}	11.2685	−0.026379	2905.5	0	0	0	0	−6685.21	0	0
K^+	Mg^{2+}	−28.2506	0.0311345	16139.0	0	0	0	0	−13262.6	0	0
K^+	Ca^{2+}	−43.804	0.0468862	23092.5	0	0	0	0	−18687.4	0	0
Na^+	$CaCl_2(aq)$	−27.3022	0	17433	0	0	0	0	0	0	0
K^+	$CaCl_2(aq)$	−24.2268	0	18665.2	0	0	0	0	0	0	0
Na^+	$MgCl_2(aq)$	0	0	−11710.7	0	0	0	0	0	0	0
K^+	$MgCl_2(aq)$	0	0	−9228.3	0	0	0	0	0	0	0
LiCl(aq)	H_2O	3.61735	0	0	0	0	0	0	0	0	0
$CaCl_2(aq)$	H_2O	−9.09197	0	0	0	0	0	0	0	0	0

Table 7 Gibbs energy of formation, entropy and heat capacity coefficients for solid phases

Solid phase	$\Delta_f G^o$	S^o	$C_p(J \cdot mol^{-1} \cdot K^{-1}) = A + B/T + C/T^2 + DT^2 + ET^3$				
	$kJ \cdot mol^{-1}$	$J \cdot mol^{-1} \cdot K^{-1}$	A	B	C	D	E
$NaNO_3$	−366.106	119.713	−493.9911	4.577221	0	−0.011965	1.0789×10^{-5}
KNO_3	−393.709	129.141	21.54	0.207936	1.02440×10^6	0	0
$Mg(NO_3)_2$	−577.191	164.000	44.7186	0.29788	7.45840×10^5	0	0
$Mg(NO_3)_2 \cdot 2H_2O$	−1101.90	183.459	228.028	0	0	0	0
$Mg(NO_3)_2 \cdot 6H_2O$	−2082.06	479.474	387.02	0	0	0	0
$Mg(NO_3)_2 \cdot 9H_2O$	−2796.09	664.176	506.264	0	0	0	0
$Ca(NO_3)_2$	−741.917	209.766	122.88	0.154009	-1.72728×10^6	0	0
$Ca(NO_3)_2 \cdot 2H_2O$	−1229.06	282.898	233.0488	0	0	0	0
$Ca(NO_3)_2 \cdot 3H_2O$	−1470.95	372.056	273.002	0	0	0	0
$Ca(NO_3)_2 \cdot 4H_2O$	−1712.6	394.4776	314.001	0	0	0	0
$NaNO_3 \cdot KNO_3$	−751.853	322.588	180.7488	0	0	0	0
$Ca(NO_3)_2 \cdot 4KNO_3$	−2331.78	836.8	515.050	0	0	0	0
LiCl	−385.531	52.206	43.74372	0.02037056	-1.60419×10^5	3.0643×10^{-7}	-9.4178×10^{-11}
$LiCl \cdot 1H_2O$	−631.728	101.838	87.4456	0	0	0	0
$LiCl \cdot 2H_2O$	−874.136	145.901	130.001	0	0	0	0
$LiCl \cdot 3H_2O$	−1114.73	198.7755	113.456	0	0	0	0
$LiCl \cdot 5H_2O$	−1592.53	337.3417	298.807	0	0	0	0
NaCl	−384.324	70.7640	47.121	0.007219	20900	1.1156×10^{-5}	0
$NaCl \cdot 2H_2O$	−858.845	164.613	130.1224	0	0	0	0
KCl	−408.548	80.5905	44.0081	0.033165	−200.0	3.5991×10^{-5}	2.285×10^{-8}
$MgCl_2 \cdot 2H_2O$	−1127.94	146.391	125.143	0.114265	0	0	0
$MgCl_2 \cdot 4H_2O$	−1627.54	249.4099	187.569	0.180038	0	0	0
$MgCl_2 \cdot 6H_2O$	−2115.67	371.4836	241.752	0.245768	0	0	0
$MgCl_2 \cdot 8H_2O$	−2593.45	466.9135	387.02	0	0	0	0
$MgCl_2 \cdot 12H_2O$	−3545.85	645.6832	546.012	0	0	0	0

Table 7 *Continued*

Solid phase	$\Delta_f G^o$ kJ·mol^{-1}	S^o J·mol^{-1}·K^{-1}	C_p(J·mol^{-1}·K^{-1}) = $A + B/T + C/T^2 + DT^2 + ET^3$				
			A	B	C	D	E
$CaCl_2$	−748.743	112.0442	72.59	0	0	0	0
$CaCl_2 \cdot 0.33H_2O$	−830.221	149.7211	83.68	0	0	0	0
$CaCl_2 \cdot 1H_2O$	−995.780	190.1758	107.947	0	0	0	0
$CaCl_2 \cdot 2H_2O$	−1248.90	212.3836	176.439	0	0	0	0
$CaCl_2 \cdot 4H_2O$	−1734.73	268.9555	245.099	0	0	0	0
$CaCl_2 \cdot 6H_2O$	−2216.93	371.4798	311.666	0	0	0	0
$KCl \cdot MgCl_2 \cdot 6H_2O$	−2530.41	443.3366	358.1504	0	0	0	0
$KCl \cdot CaCl_2$	−1174.68	202.8495	124.683	0	0	0	0
$2MgCl_2 \cdot CaCl_2 \cdot 12H_2O$	−5004.54	910.9154	689.1048	0	0	0	0
$MgCl_2 \cdot 2CaCl_2 \cdot 6H_2O$	−3644.62	637.0014	455.6376	0	0	0	0
$CaCl_2 \cdot Ca(NO_3)_2 \cdot 4H_2O$	−2480.47	386.6016	386.6016	0	0	0	0
H_2O(s)	−236.588	44.77926	5.9304	0.119641	−69543.7	0	0

taken from Refs. [16, 17] without any change. On the other hand, the standard-state properties of the ion pairs have been adjusted based on the multi-property regressions. Table 6 shows the binary parameters used in the ionic interaction term, Eqs. 6 and 7. The number of coefficients used to express the temperature dependence of the ion interaction term depends on the temperature range and accuracy of the available experimental data. Thus, a fairly complex temperature dependence is used for the cation-anion parameters that reflects the properties of salts whose properties are well known. On the other hand, other parameters are calculated using a simpler temperature dependence. Finally, Table 7 summarizes the properties of all solid phases that were included in the model. These properties were used to calculate the chemical potential of the solids according to standard thermodynamics.

5 Results and Discussion

In this section, we compare the modeling results with experimental data for all constituent binary subsystems and selected ternary and higher-order systems. First, we focus on solubility relationships for the binary and ternary systems. Then, we analyze vapor-liquid equilibrium data for solid-saturated ternary systems using literature data [7]. Finally, we apply the model to the new isopiestic data and analyze them in the light of solid–liquid equilibrium predictions obtained from the model.

5.1 Solid–Liquid Equilibria in Binary Systems

Figures 1–8 show the calculated and experimental solid–liquid equilibria for the eight binary subsystems for temperatures up to approximately 300 °C. In all cases, the SLE diagrams include the solubility of ice (denoted by $H_2O(s)$) in a salt solution. The lowest temperature in each diagram corresponds to the eutectic point, at which ice coexists with the anhydrous or hydrated salt that is stable at the lowest temperature. Then, solubility curves are included for all solid forms that are stable up to 300 °C.

It is evident that the complexity of the solubility behavior depends primarily on whether the cation belongs to the first group of the periodic table (Na, K) or the second (Mg, Ca). The sodium salts show relatively simple solid–liquid equilibrium patterns. As shown in Figs. 1

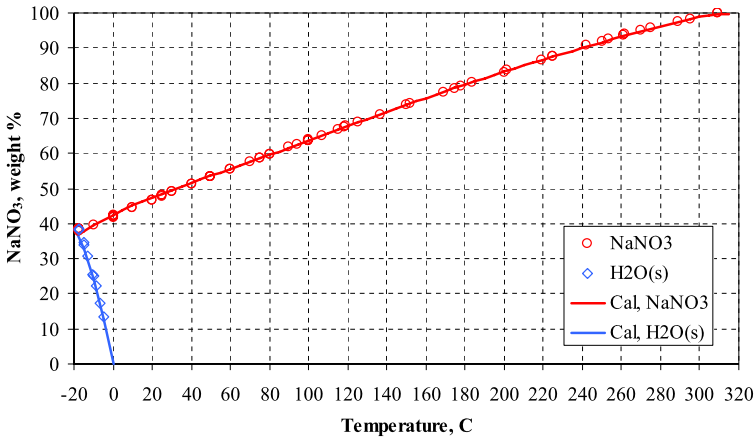

Fig. 1 Calculated and experimental solid–liquid equilibria in the binary system $NaNO_3$–H_2O

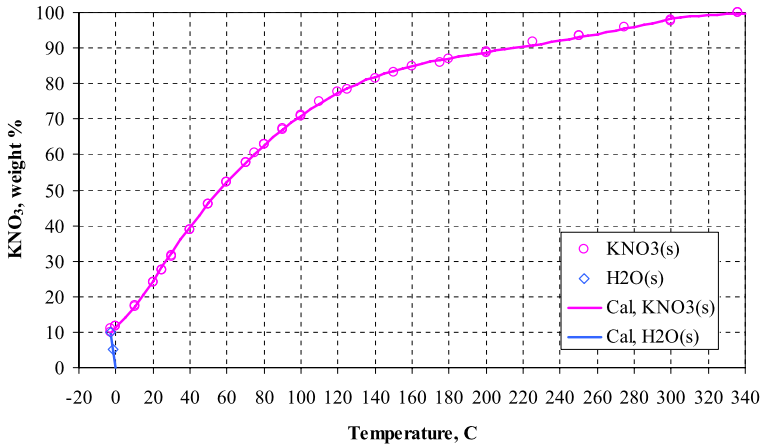

Fig. 2 Calculated and experimental solid–liquid equilibria in the system KNO_3–H_2O

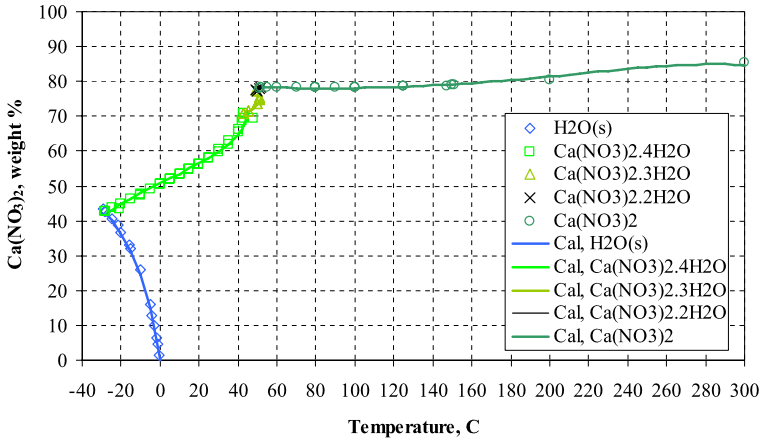

Fig. 3 Calculated and experimental solid–liquid equilibria in the system $Ca(NO_3)_2$–H_2O

and 2, $NaNO_3$ and KNO_3 form only one, anhydrous, solid precipitate at temperatures from sub-zero to ca. 300 °C. In both cases, the solubility continuously increases with temperature up to the melting point of the pure solid. It is noteworthy that the model accurately reproduces the solubility up to the melting point. Unlike $NaNO_3$ and KNO_3, the nitrates of calcium and magnesium form more than one stable solid phase. This is illustrated in Figs. 3 and 4, which show the stability ranges for the various hydrated and anhydrous forms of $Ca(NO_3)_2$ and $Mg(NO_3)_2$, respectively. The solubility behavior is particularly noteworthy for $Mg(NO_3)_2$ (Fig. 4). In the case of this binary, the $Mg(NO_3)_2 \cdot 6H_2O$ phase melts congruently, which results in a solubility maximum. Thus, in the temperature range from ca. 45 to 90 °C, the salt has three values of solubility, i.e., two for $Mg(NO_3)_2 \cdot 6H_2O$ on both sides of the solubility maximum and one for $Mg(NO_3)_2 \cdot 2H_2O$ at higher salt concentrations. The solubility behavior of chlorides (Figs. 5–8) essentially parallels that of the nitrates with respect to the complexity of their phase behavior. However, the solubility of the chlorides is

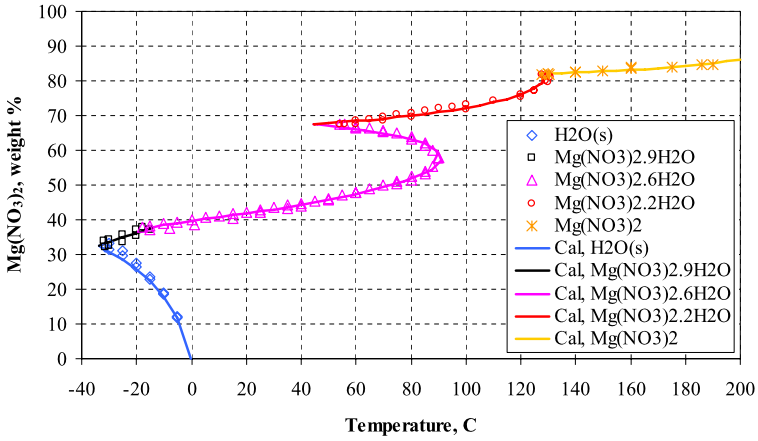

Fig. 4 Calculated and experimental solid–liquid equilibria in the system $Mg(NO_3)_2$–H_2O

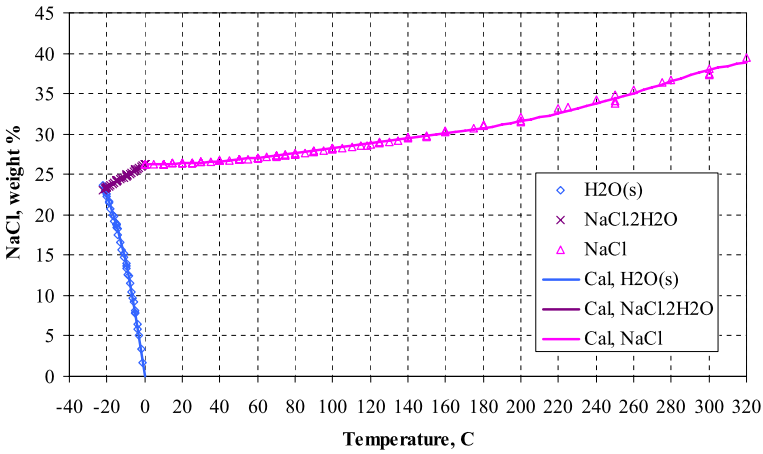

Fig. 5 Calculated and experimental solid–liquid equilibria in the system NaCl–H_2O

substantially lower than that of the nitrates. Similarly to the corresponding nitrates, sodium and potassium chlorides form only one stable anhydrous solid phase at the temperatures of interest. The only exception is the hydrate $NaCl{\cdot}2H_2O$, which is stable only below 0 °C (cf. Fig. 5). The chlorides of calcium and magnesium form a series of stable hydrates as shown in Figs. 7 and 8, respectively. For all binary subsystems, the model reproduces the measurements essentially within the scatter of experimental data.

5.2 Solid–Liquid Equilibria in Ternary Systems

Figures 9–15 show solid–liquid equilibrium diagrams for seven representative ternary systems. In these figures, solubility isotherms are plotted using the weight percent of both salts as independent variables. Thus, the points on the individual salt concentration axes correspond to solubilities in the binary subsystems. In general, the chemical identity of the stable

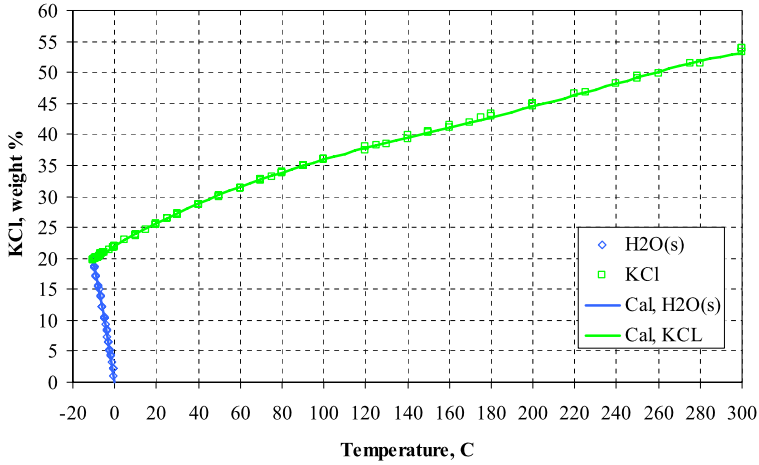

Fig. 6 Calculated and experimental solid–liquid equilibria in the system KCl–H_2O

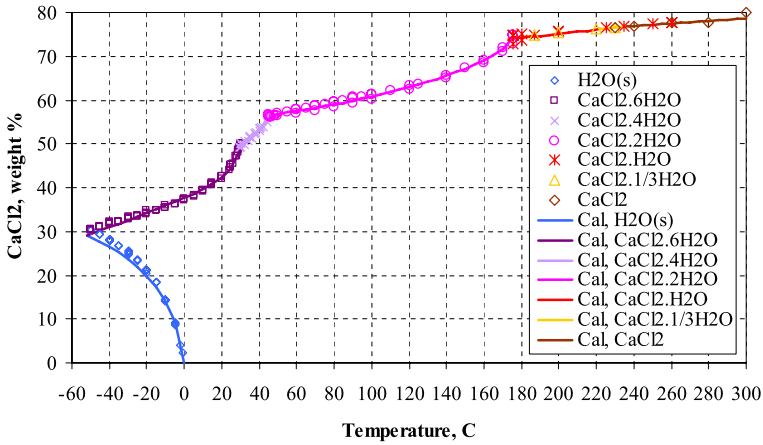

Fig. 7 Calculated and experimental solid–liquid equilibria in the system $CaCl_2$–H_2O

solid phase may vary with the overall composition of the system and may not be the same as in the binary subsystems. Therefore, the solid phases that are in equilibrium with saturated solutions are marked next to the solubility curves in Figs. 9–15.

Figure 9 shows the solubility behavior in the ternary system $NaNO_3$–$Ca(NO_3)_2$–H_2O. In this case, the diagram is fairly simple because the stability of the solid phases that precipitate for the constituent binary subsystems persists in the ternary system. Thus, the diagram shows two branches that extend from the solubility points for the binary subsystems. These two branches correspond to the precipitation of $NaNO_3$ and $Ca(NO_3)_2 \cdot 4H_2O$ or $Ca(NO_3)_2$, depending on the temperature. The solubility behavior of the $Mg(NO_3)_2$–$Ca(NO_3)_2$–H_2O system (Fig. 10) is qualitatively similar in that the identity of the stable phases does not change by moving from the binary subsystems to the ternary. However, the relative stability of the magnesium and calcium salts strongly changes with temperature. For example, $Ca(NO_3)_2 \cdot 4H_2O$ precipitates over a wide range of conditions at lower temperatures whereas

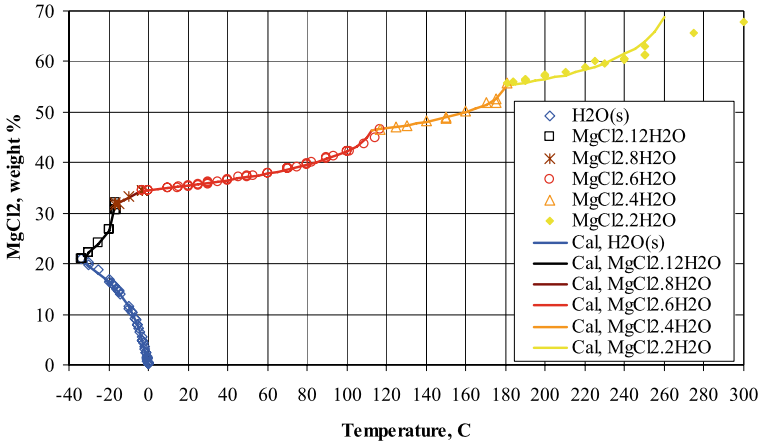

Fig. 8 Calculated and experimental solid–liquid equilibria in the system $MgCl_2$–H_2O

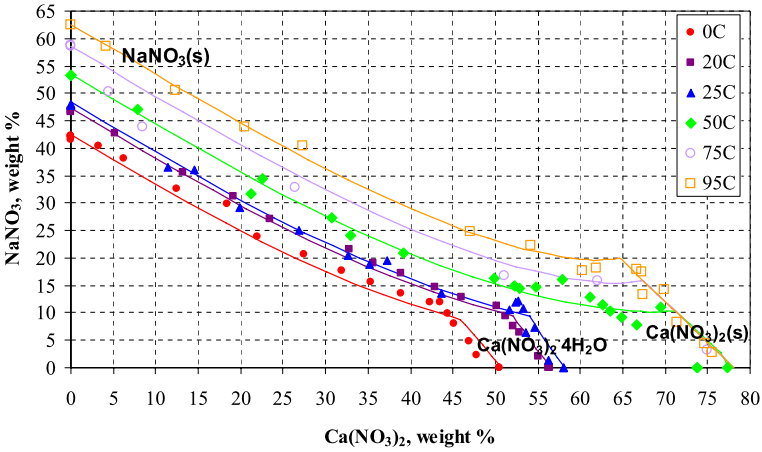

Fig. 9 Calculated and experimental solubilities of solids in the system $NaNO_3$–$Ca(NO_3)_2$–H_2O

the stability range of $Ca(NO_3)_2 \cdot 3H_2O$ is very narrow at 50 °C and is limited to a region close to the binary axis.

Figure 11 illustrates solid–liquid equilibria for the $NaNO_3$–KNO_3–H_2O system. In this case, simple solubility behavior is observed at low and moderate temperatures (up to ca. 150 °C). However, a solid solution phase appears at higher temperatures and manifests itself as two breaks in the solubility isotherms at 175 and 200 °C. This solid phase is tentatively identified as $NaNO_3 \cdot KNO_3$.

Figures 12–15 show the behavior of mixed nitrate-chloride ternaries. The solubility isotherms for the NaCl–$NaNO_3$–H_2O (Fig. 12) and KCl–KNO_3–H_2O (Fig. 13) ternaries show simple solubility behavior without a phase change on moving from the binaries to the ternary. However, the $MgCl_2$–$Mg(NO_3)_2$–H_2O system shows a very complicated solubility pattern as shown in Fig. 14. This pattern results partly from the presence of a congruently melting solid phase, $Mg(NO_3)_2 \cdot 6H_2O$, in the binary subsystem $Mg(NO_3)_2$–H_2O. Because

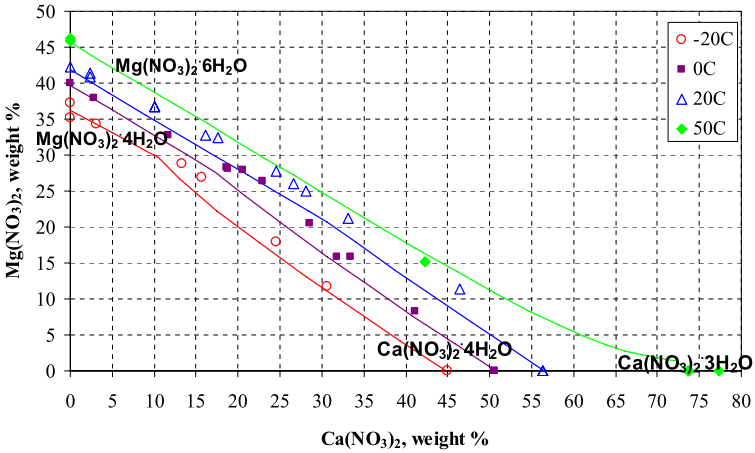

Fig. 10 Calculated and experimental solid–liquid equilibria in the system $Mg(NO_3)_2$–$Ca(NO_3)_2$–H_2O

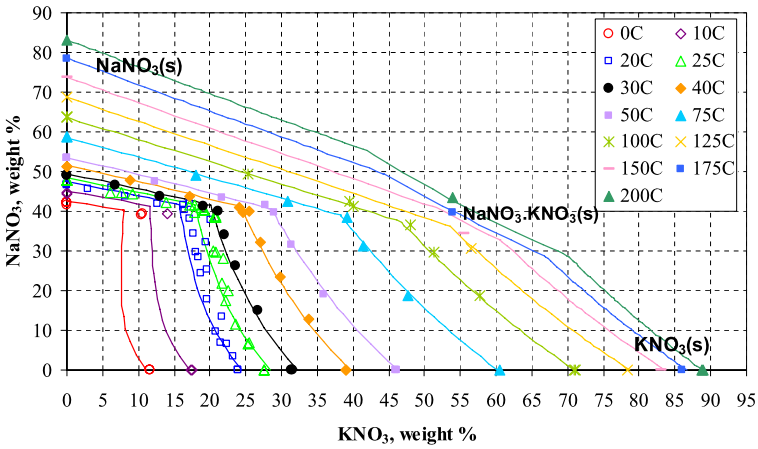

Fig. 11 Calculated and experimental solubilities of solids in the system $NaNO_3$–KNO_3–H_2O

of this, the solubility of $Mg(NO_3)_2 \cdot 6H_2O$ forms a loop in the ternary phase diagram at intermediate temperatures. In addition to the loop, an additional solubility curve is observed that connects the solubilities of $MgCl_2 \cdot 6H_2O$ and $Mg(NO_3)_2 \cdot 6H_2O$ in the binary subsystems. At higher temperatures, the solubility loop disappears. However, the solubility behavior is further complicated by the transition of the stable solid form from $MgCl_2 \cdot 6H_2O$ to $Mg(NO_3)_2 \cdot 2H_2O$ through $MgCl_2 \cdot 4H_2O$ and then $MgCl_2 \cdot 2H_2O$. These transitions are visible in the solubility curves as characteristic break points. It is noteworthy that this complex phase behavior is accurately reproduced by the model.

The ternary system NaCl–KNO_3–H_2O is shown in Fig. 15. In this case, simple solubility behavior is observed at temperatures up to ca. 50 °C. However, a different phase, KCl, appears at higher temperatures.

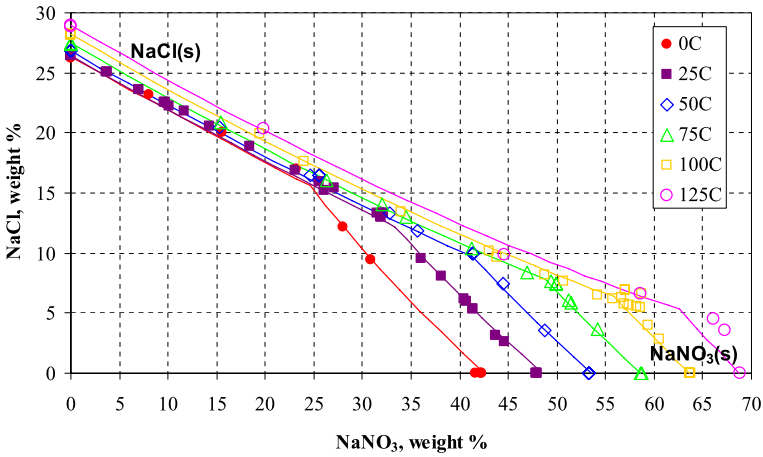

Fig. 12 Calculated and experimental solid–liquid equilibria in the system NaCl–$NaNO_3$–H_2O

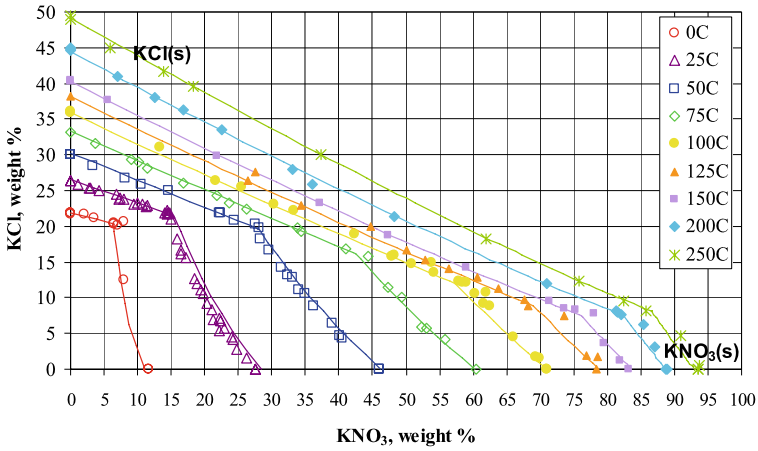

Fig. 13 Calculated and experimental solid–liquid equilibria in the system KCl–KNO_3–H_2O

5.3 Water Activities in Saturated Solutions

Vapor pressures of saturated solutions are of particular interest for studying deliquescence. The vapor pressures are determined by the activity of water. At solid saturation, a minimum of the water activity and, hence, vapor pressure, is reached for a given salt composition. Figures 16–21 show the experimental and calculated water activities and the corresponding concentrations of ions in saturated solutions of two mixed salts in water. In these figures, the composition of a mixture of salt A and salt B is expressed using mole fractions on a water-free basis, i.e., $x'_A = n_A/(n_A + n_B)$ where n_A and n_B are the numbers of moles of salts A and B. Each of the ternary mixtures contains water in the amount that is necessary to achieve solid–liquid saturation. The overall compositions (including water) of the mixtures in Figs. 16–21 are consistent with those shown in the corresponding ternary solid–liquid equilibrium diagrams. By plotting the water activities on a water-free basis, it is easy to

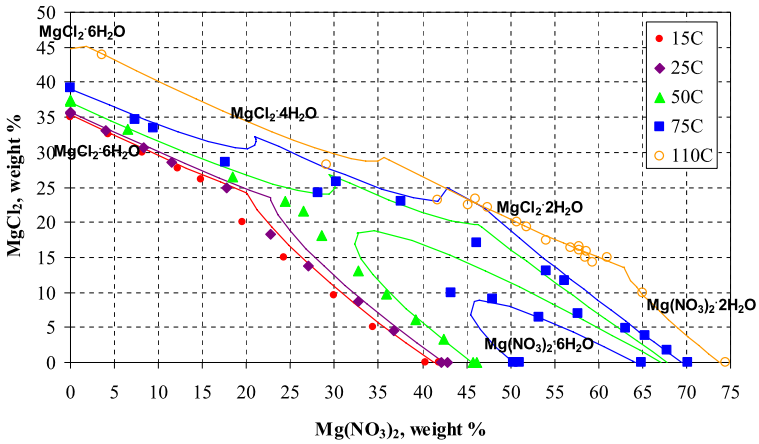

Fig. 14 Calculated and experimental solid–liquid equilibria in the system $MgCl_2$–$Mg(NO_3)_2$–H_2O

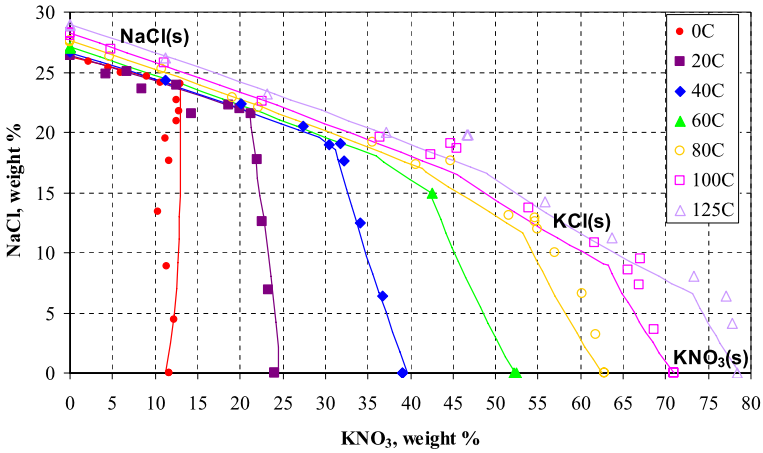

Fig. 15 Calculated and experimental solid–liquid equilibria in the system NaCl–KNO_3–H_2O

see how the activity changes as one salt is gradually replaced with another in a saturated solution.

Figure 16 represents the water activity in the $NaNO_3$–NaCl–H_2O system as the overall composition varies from pure $NaNO_3$ to pure NaCl. The solid phases that are in equilibrium with the saturated solutions are indicated next to the vapor pressure curves. These solid phases are consistent with the SLE diagram for the same system, which is shown in Fig. 12. The minimum in the water activity is reached at the eutonic point, at which both NaCl(s) and $NaNO_3$(s) coexist. The model predicts the eutonic point with very good accuracy. As shown in Fig. 17, the model also accurately predicts the equilibrium concentrations of the Na^+, Cl^- and NO_3^- ions along the solid saturation line. This provides an additional confirmation of the SLE diagram (cf. Fig. 12). The water activities in the system $NaNO_3$–KNO_3–H_2O show a very similar pattern as illustrated in Fig. 18. The corresponding concentrations of ions at saturation are shown in Fig. 19.

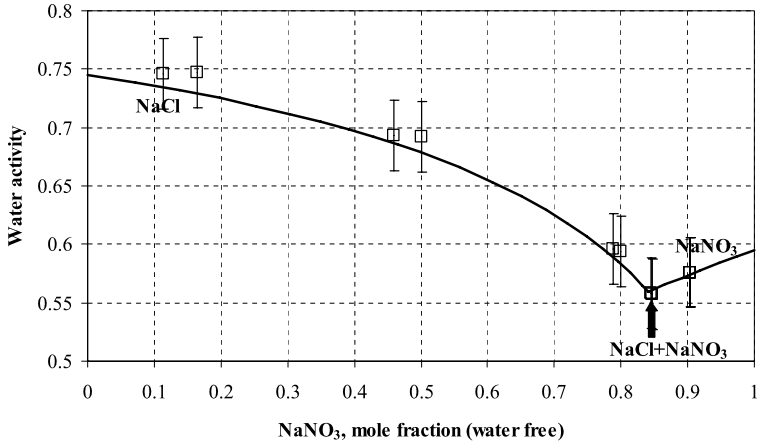

Fig. 16 Calculated and experimental activity of water in solutions saturated with mixtures of $NaNO_3$ and NaCl at 90 °C with varying compositions. The solid phases that coexist with the saturated solutions are indicated along the water activity curve. The data are from Carroll et al. [7]

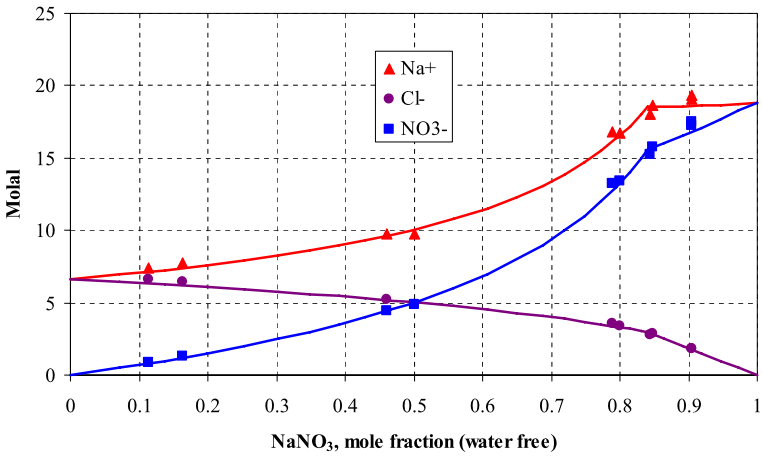

Fig. 17 Concentrations of ions in the system $NaNO_3$–NaCl–H_2O along the solid–liquid saturation line at 90 °C. The data are from Carroll et al. [7]

The system NaCl–KNO_3–H_2O (Figs. 20, 21) exhibits a somewhat more complex behavior although the experimentally observed patterns are partially obscured by higher experimental uncertainties for this mixture. In this case, the vapor pressure curve shows two break points, which correspond to the transition from KNO_3(s) to KCl(s) and then from KCl(s) to NaCl(s) as sodium nitrate is progressively replaced by sodium chloride in the saturated solution. This transition is consistent with the SLE diagram in Fig. 15. The predicted water activities (Fig. 20) and equilibrium ionic compositions (Fig. 21) agree with the data within the experimental uncertainty.

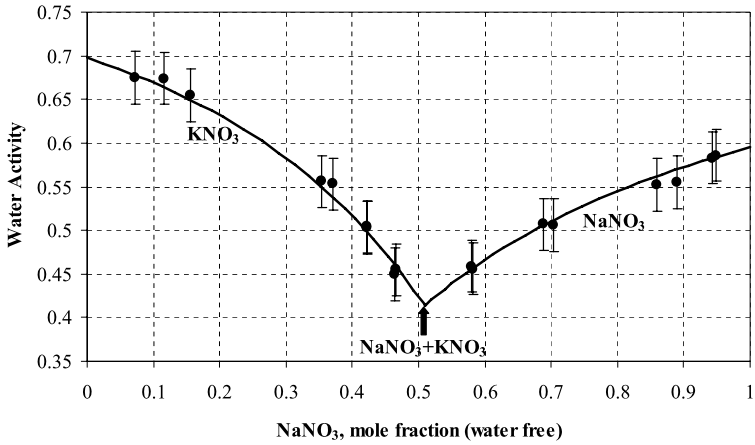

Fig. 18 Calculated and experimental [7] activity of water in solutions saturated with mixtures of $NaNO_3$ and KNO_3 with varying compositions at 90 °C. The solid phases that coexist with the saturated solutions are indicated along the water activity curve

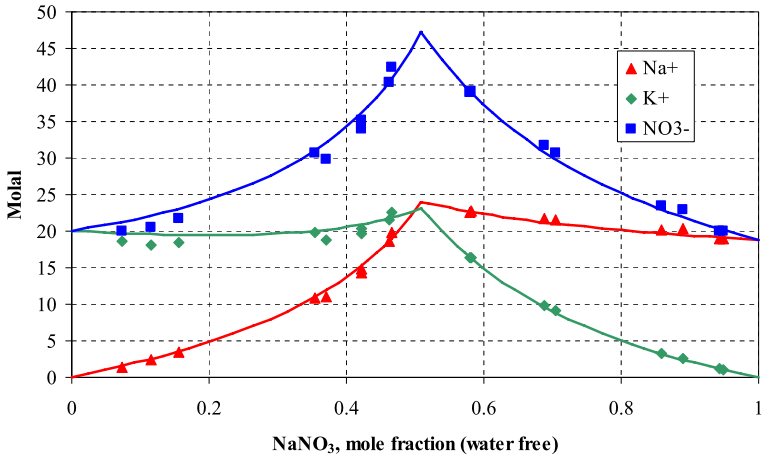

Fig. 19 Concentrations of ions in the system $NaNO_3$–KNO_3 along the solid–liquid saturation line at 90 °C. The data are from Carroll et al. [7]

5.4 Comparison with the New Isopiestic Data

The isopiestic measurements reported here simultaneously reflect two fundamental properties of the system: the activity of water as a function of solution concentration and the occurrence of solid–liquid transitions. Thus, the isopiestic data provide a stringent test of the model's capability to represent simultaneously the vapor-liquid and solid–liquid equilibria. Figures 22–26 compare the calculated and experimental water activities (upper diagrams) and osmotic coefficients (lower diagrams) for the systems defined in Table 1. While the water activity is of direct interest for studying deliquescence, osmotic coefficients are more convenient for analyzing the data, in particular at lower concentrations. This is due to

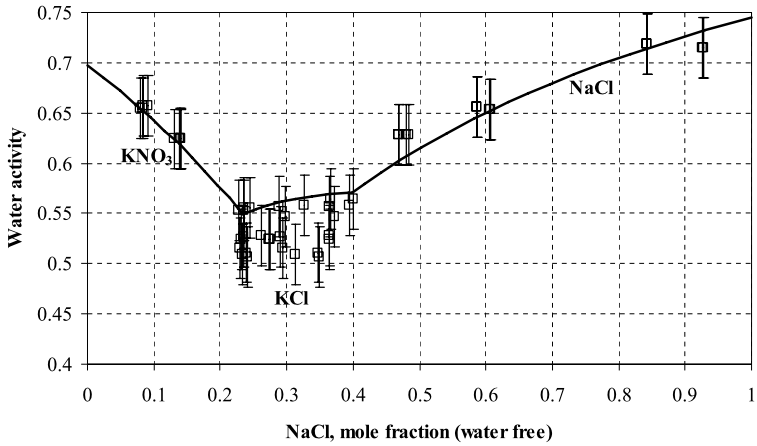

Fig. 20 Calculated and experimental [7] activity of water in solutions saturated with mixtures of NaCl and KNO_3 with varying compositions at 90 °C. The solid phases that coexist with the saturated solutions are indicated along the water activity curve

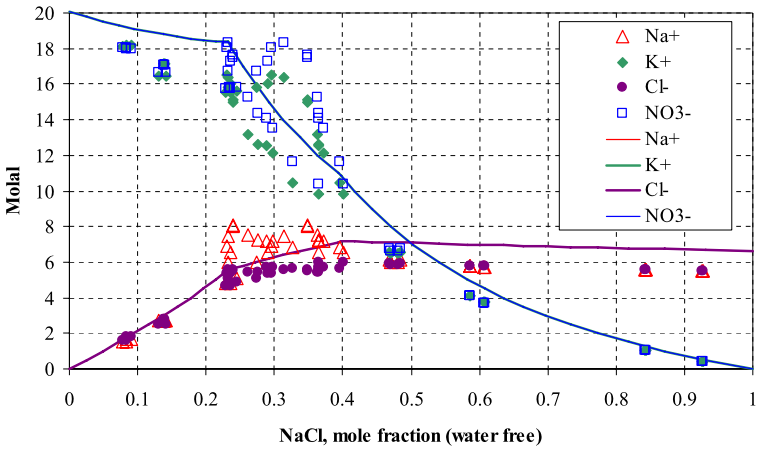

Fig. 21 Concentrations of ions in the system NaCl–KNO_3–H_2O [7] along the solid–liquid saturation line at 90 °C

a stronger variability of osmotic coefficients at lower concentrations, at which water activities do not differ much from unity.

The systems in Figs. 22–26 have been grouped according to their increasing complexity. In all cases, calculations were performed by increasing the total apparent mole fraction of the salt from zero (or reducing the apparent mole fraction of water from one) while keeping the ratios of the various salts as defined in Table 1. Here, the apparent mole fraction is defined by including the salts and water in both the solution and in the various solid phases that may precipitate. The apparent mole fraction is identical to the mole fraction in the solution only if there is no solid phase in the system. Once a solid phase precipitates, the plot of water activity or osmotic coefficient against the apparent mole fraction exhibits a change in slope due to the appearance of a solid phase. The points at which new solid phases start

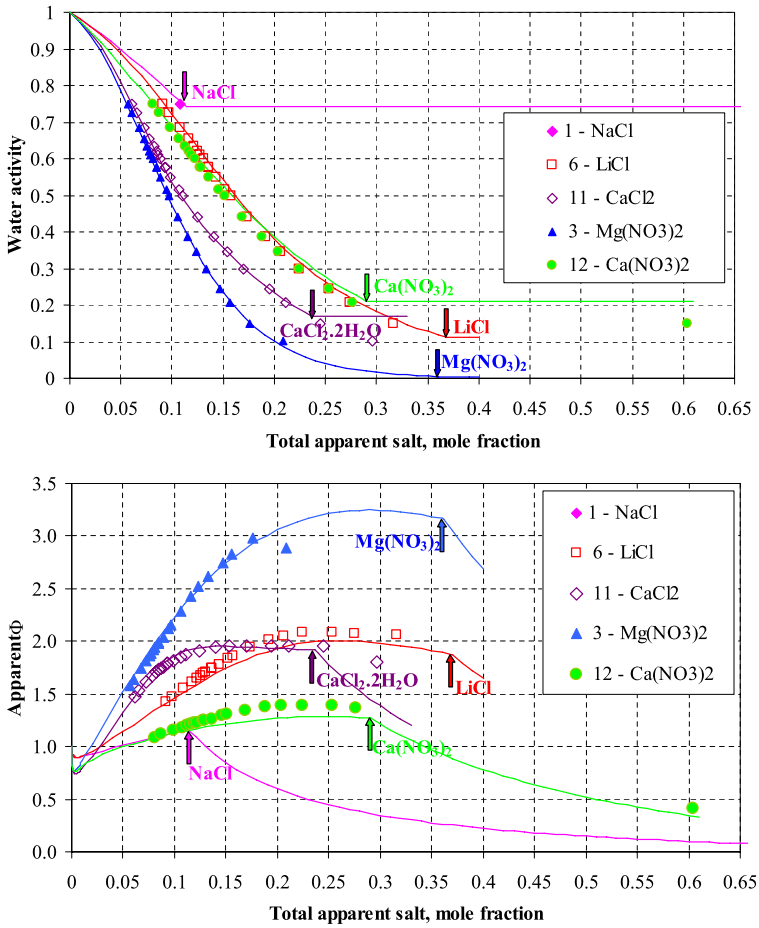

Fig. 22 Calculated and experimental water activities (**upper diagram**) and osmotic coefficients (**lower diagram**) of single-salt systems at 140 °C. The *system numbers* correspond to the solutions defined in Table 1. The *arrows* indicate the total system composition at which a given solid phase is predicted to precipitate

to precipitate are shown by arrows in Figs. 22–26 and the compositions of the solids are indicated next to the arrows. It should be noted that the solids identified in the plots have been determined from the thermodynamic model. The isopiestic measurements do not provide information on the chemical identity of the solid phase. The breaks are typically more pronounced on the osmotic coefficient plots, especially at lower concentrations. Starting at the precipitation point, the apparent mole fraction ceases to be equivalent to the solution composition and the calculated water activity starts to reflect the property of a solid–liquid assembly.

First, Fig. 22 summarizes the results of calculations for simple binary solutions containing NaCl, $Mg(NO_3)_2$, LiCl, $CaCl_2$ and $Ca(NO_3)_2$ (samples 1, 3, 6, 11 and 12 in Table 1). Once a solid phase precipitates (as indicated by the vertical arrows), the water activity becomes constant. This is a consequence of the phase rule. The constant water activities are shown as horizontal portions of the curves in Fig. 22. Since the model was calibrated using extensive experimental data for binary systems (cf. Table 3), the obtained agreement

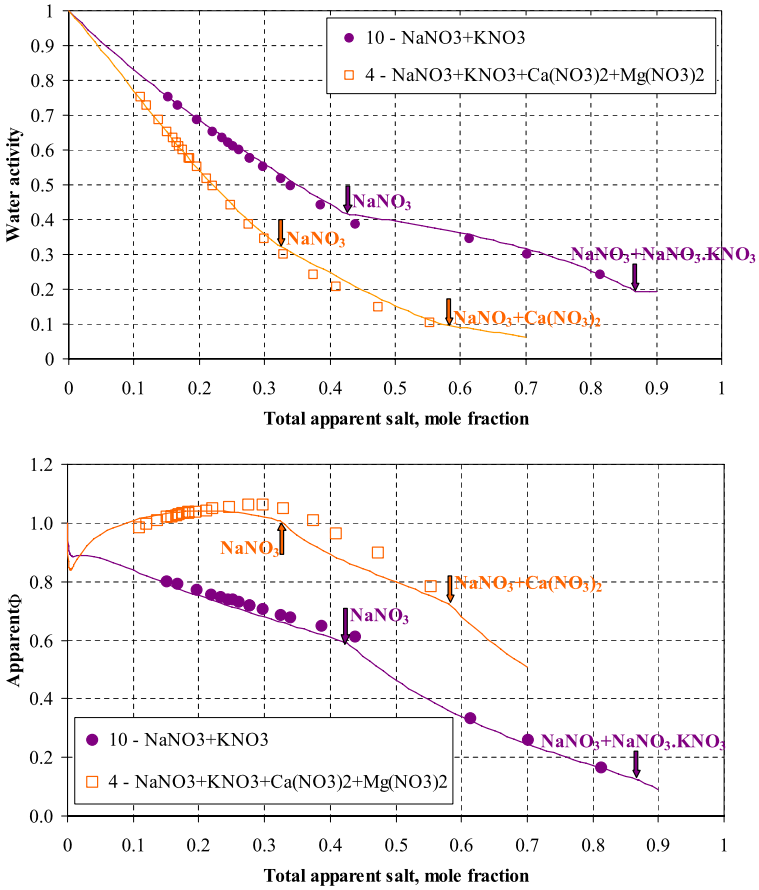

Fig. 23 Calculated and experimental water activities (**upper diagram**) and osmotic coefficients (**lower diagram**) for two systems containing the nitrates of Na, K, Ca, and Mg at 140 °C. The *system numbers* correspond to the solutions defined in Table 1. The *arrows* indicate the total apparent salt mole fraction at which a given solid phase is predicted to precipitate

between the calculations and experimental data is not surprising and simply verifies the consistency of the new isopiestic data with earlier thermodynamic data for the binary systems.

The differences in osmotic coefficients between the new experimental data and the present model for LiCl and $Ca(NO_3)_2$, reaching 0.12, or nearly 10% for the latter, appear to be larger than expected for binary systems. However, in contrast to lower temperature data, at temperatures above 373.15 K and at high concentrations, especially for hygroscopic compounds, differences of several percent between sets of osmotic coefficient data are rather typical. Due to the difficulty, and hence the scarcity of vapor pressure measurements by any method at these conditions, the model equations depend strongly on the quality of the few best literature data sets. Notable sources of experimental error include water and other impurity content in the salts, and the presence carbon dioxide and other non-condensable gases. Whereas the water activities used in this work were obtained using our recent thermodynamic model [5] for aqueous $CaCl_2$ as the reference, the present model was not revised

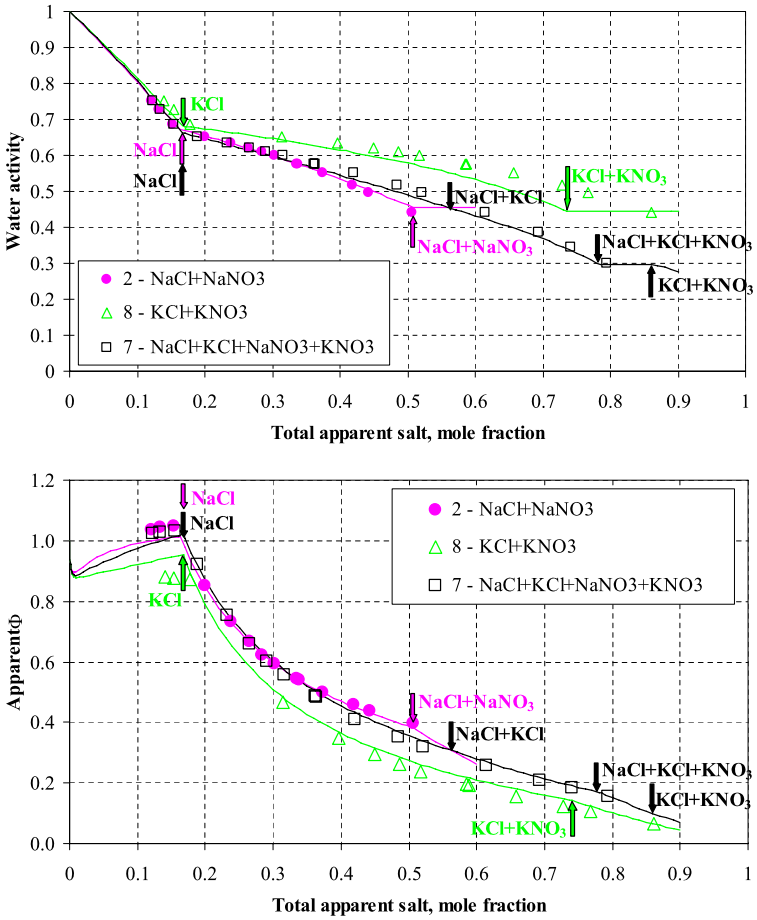

Fig. 24 Calculated and experimental water activities (**upper diagram**) and osmotic coefficients (**lower diagram**) for three systems containing various combinations of the Na^+, K^+, NO_3^- and Cl^- ions at 140 °C. The *system numbers* correspond to the solutions defined in Table 1. The *arrows* indicate the total apparent salt mole fraction at which a given solid phase is predicted to precipitate

to include these results. In addition, there were small deviations between water activities and osmotic coefficients calculated using (a) $CaCl_2$ reference, (b) LiCl reference, and (c) direct pressure measurements. The largest difference between the osmotic coefficients for LiCl calculated using the $CaCl_2$ reference [5] and those calculated using directly measured pressures was 0.052 at 25.7 mol·kg^{-1} (the average difference was 0.021). The difference between the LiCl model used in this work and our earlier unpublished results exceeds 0.05 even at much lower molality (7 mol·kg^{-1}). Thus, we conclude that the discrepancy between the measured and calculated osmotic coefficients seen in Fig. 22 is the result of a somewhat unfortunate combination of experimental errors inherent in both the present results and the representation of earlier literature results.

A more stringent test of the model is provided by the multicomponent systems. Figure 23 shows the results for two systems containing only nitrates, i.e., the ternary system $NaNO_3$–KNO_3–H_2O (sample 10) and the quinary mixture $NaNO_3$–KNO_3–$Ca(NO_3)_2$–$Mg(NO_3)_2$–

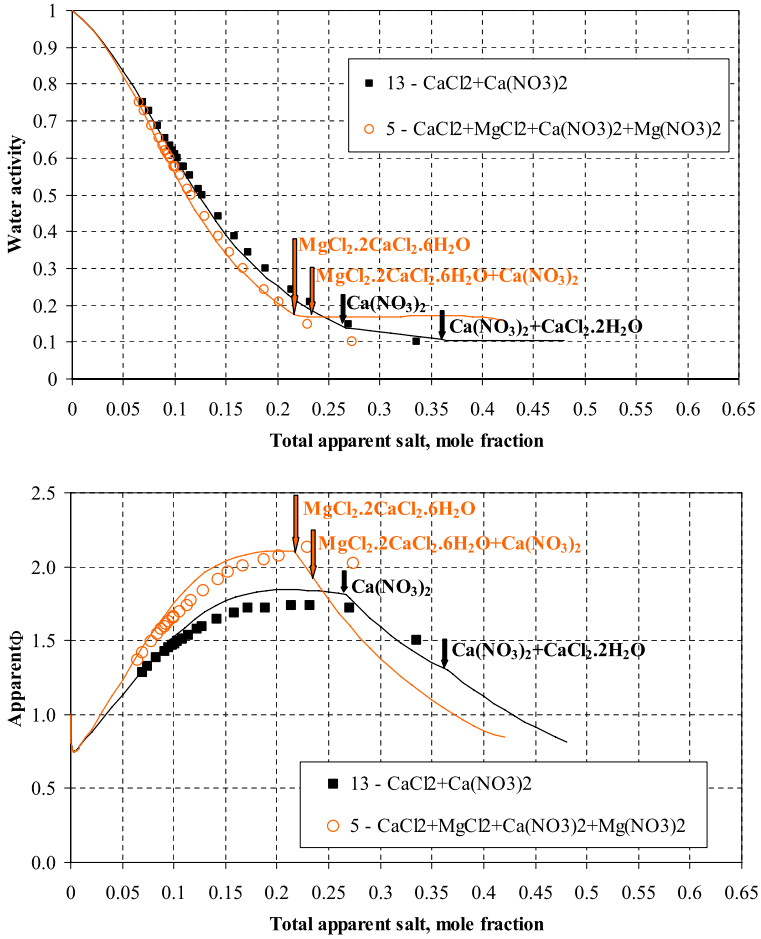

Fig. 25 Calculated and experimental water activities (**upper diagram**) and osmotic coefficients (**lower diagram**) for two systems containing the Ca^{2+}, Mg^{2+}, Cl^- and NO_3^- ions at 140 °C. The *system numbers* correspond to the solutions defined in Table 1. The *arrows* indicate the total apparent salt mole fraction at which a given solid phase is predicted to precipitate

H_2O (sample 4). In ternary and higher-order systems, precipitation of a solid phase does not lead to a constant value of water activity. Instead, a change in slope is observed. In the case of these two nitrate systems, two discontinuous slope changes occur. The first one is associated with the transition from a one-phase to a two-phase (i.e., liquid + $NaNO_3$(s)) system and the second one reflects a change from a two-phase to a three-phase system as indicated by the arrows in Fig. 23. The model accurately predicts the water activities including the change in slope and the exact composition of the system at which the transition occurs. Thus, the model makes it possible to identify the phases that precipitate as the total salt fraction is increased.

Figure 24 groups the results for three systems containing chlorides and nitrates of sodium and potassium (samples 2, 7 and 8). As with the nitrate-only systems, the water activities and the accompanying phase transitions are accurately predicted by the model. The transitions

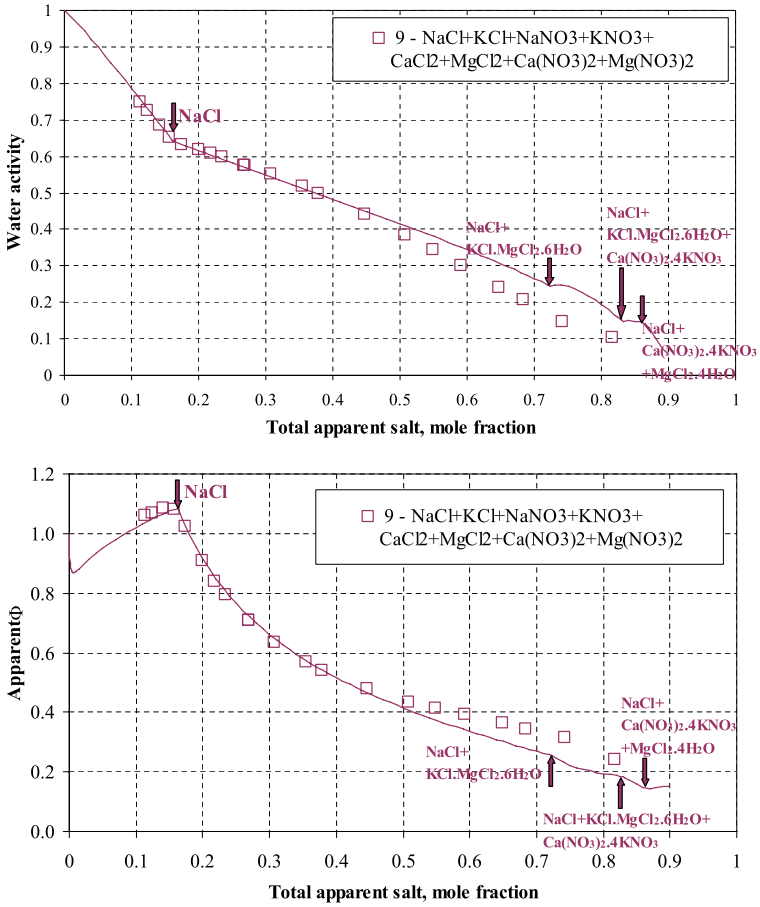

Fig. 26 Calculated and experimental water activities (**upper diagram**) and osmotic coefficients (**lower diagram**) for a system containing a combination of the Na^+, K^+, Ca^{2+}, Mg^{2+}, Cl^- and NO_3^- ions at 140 °C. The solution is defined in Table 1. The arrows indicate the total apparent salt mole fraction at which a given solid phase is predicted to precipitate

for the quaternary system $NaCl–NaNO_3–KNO_3–H_2O$ appear to be particularly complex. In this case, the system transitions from a liquid to a liquid + NaCl(s) mixture, then to liquid + NaCl(s) + KCl(s), then to liquid + NaCl(s) + KCl(s) + KNO_3(s) and, finally, to liquid + KCl(s) + KNO_3(s). Figure 25 shows the results for mixed chloride–nitrate systems containing calcium and magnesium rather than sodium and potassium. Water activity drops to substantially lower values in calcium and magnesium salts before saturation is achieved. In this case, saturation results in the formation of hydrated double salts such as $MgCl_2 \cdot 2CaCl_2 \cdot 6H_2O$. As with the Na–K–Cl–$NO_3$ system, transitions of the type liquid → liquid + solid A are followed by transitions of the type liquid + solid A → liquid + solid A + solid B. The predicted water activities are in very good agreement with the data.

Finally, Fig. 26 shows the results for a six-component system that contains all ions that are the subject of this study (i.e., Na^+, K^+, Ca^{2+}, Mg^{2+}, Cl^- and NO_3^-). As indicated in

Table 1, the mixture was actually made from eight salts in addition to water (i.e., NaCl, KCl, $NaNO_3$, KNO_3, $CaCl_2$, $MgCl_2$, $Ca(NO_3)_2$ and $Mg(NO_3)_2$). However, the system contains six independent components in the sense of the phase rule. Because of its complexity, this system exhibits four transitions as indicated by the vertical arrows in Fig. 26. At very high total apparent salt fractions (above ca. 0.6), the predicted water activities are somewhat less accurate, which might indicate that a different solid phase precipitates at some conditions (possibly a double or triple salt that does not occur in simpler systems).

6 Conclusions

A comprehensive model has been established for calculating the thermodynamic properties of Na–K–Mg–Ca–Cl–NO_3 systems. The parameters of the model have been determined using a combination of an extensive literature database and new isopiestic measurements that provide important information for multicomponent systems at elevated temperatures (140 °C).

The experimental method based on the use of the ORNL gravimetric isopiestic apparatus allows for the detection of solid phase precipitation and therefore a definitive determination of complete relative humidity versus composition phase diagrams. For salt mixtures several samples are needed to cover the entire range of compositions, however, one sample is sufficient for determination of the mixture deliquescence *RH*.

The model has been shown to provide accurate predictions of thermodynamic properties in wide ranges of temperature (from the freezing point to 300 °C) and concentration (from infinite dilution to the melting point). In particular, the model comprehensively reproduces solid–liquid equilibria and water activities in binary, ternary and higher-order systems. Also, the model accurately reproduces the new isopiestic data, including the changes in the slope of water activity versus the total salt mole fraction. These changes in the slope reflect the precipitation of various solid phases, thus providing a stringent test for the model.

The Na–K–Mg–Ca–Cl–NO_3 mixtures provide a good approximation of the behavior of deliquescing systems. Among the common anions that occur in nature, chlorides are the most important aggressive species and nitrates are important inhibitors in the corrosion of nickel-base alloys and stainless steels. Thus, the concentration of chlorides and nitrates is particularly important for predicting materials performance. Compared with the Cl^- and NO_3^- ions, other anions (e.g., hydroxides and carbonates) are expected to occur in lower concentrations in deliquescing systems. Most of the other oxygen-containing anions have weak inhibitive properties. However, their inhibitive behavior is much less pronounced than that of nitrates and, therefore, their role in corrosion phenomena is less significant. Whereas the inclusion of anions such as OH^-, CO_3^{2-} and SO_4^{2-} is beyond the scope of this study, the mixed-solvent electrolyte model can be relatively easily extended to achieve a more general coverage of solution chemistry.

Acknowledgements The financial support of this work from the Science & Technology Program of the Office of Science and Technology and International (OST&I), Office of Civilian Radioactive Waste Management (OCRWM), U. S. Department of Energy (DOE) is gratefully acknowledged. This work was carried out by United States Department of Energy, under contract DE-AC05-00OR22725, Oak Ridge National Laboratory, managed and operated by UT-Battelle, LLC. The interactions among investigators in the OST&I Materials Performance Thrust are appreciated and gratefully acknowledged.

References

1. Holmes, H.F., Baes Jr., C.F., Mesmer, R.E.: Isopiestic studies of aqueous solutions at elevated temperatures I. KCl, $CaCl_2$, and $MgCl_2$. J. Chem. Thermodyn. **10**, 983–996 (1978)
2. Holmes, H.F., Baes Jr., C.F., Mesmer, R.E.: Isopiestic studies of aqueous solutions at elevated temperatures II. NaCl + KCl Mixtures. J. Chem. Thermodyn. **11**, 1035–1050 (1979)
3. Holmes, H.F., Mesmer, R.E.: Thermodynamic properties of aqueous solutions of the alkali metal chlorides to 250 °C. J. Phys. Chem. **87**, 1242–1255 (1983)
4. Rard, J.A., Platford, R.F.: In: Pitzer, K.S. (Ed.) Activity Coefficients in Electrolyte Solutions, 2nd edn., pp. 209–277. CRC Press, Boca Raton (1991)
5. Gruszkiewicz, M.S., Simonson, J.M.: Vapor pressures and isopiestic molalities of concentrated $CaCl_2$(aq), $CaBr_2$(aq), and NaCl(aq) to $T = 523$ K. J. Chem. Thermodyn. **37**, 906–930 (2005)
6. Ge, Z., Wexler, A.S., Johnston, M.V.: Deliquescence behavior of multicomponent aerosols. J. Phys. Chem. A **102**, 173–180 (1998)
7. Carroll, S., Craig, L., Wolery, T.J.: Deliquescence of NaCl–$NaNO_3$, KNO_3–$NaNO_3$, and NaCl–KNO_3 salt mixtures from 90 to 120 °C. Geochim. Trans. **6**, 19–30 (2005)
8. Wang, P., Anderko, A., Young, R.D.: A speciation-based model for mixed-solvent electrolyte systems. Fluid Phase Equilib. **203**, 141–176 (2002)
9. Wang, P., Springer, R.D., Anderko, A., Young, R.D.: Modeling phase equilibria and speciation in mixed-solvent electrolyte systems. Fluid Phase Equilib. **222–223**, 11–17 (2004)
10. Wang, P., Anderko, A., Springer, R.D., Young, R.D.: Modeling phase equilibria and speciation in mixed-solvent electrolyte systems II. Liquid–liquid equilibria and properties of associating electrolyte solutions. J. Mol. Liq. **125**, 37–44 (2006)
11. Pitzer, K.S.: Electrolytes. From dilute solutions to fused salts. J. Am. Chem. Soc. **102**, 2902–2906 (1980)
12. Abrams, D.S., Prausnitz, J.M.: Statistical thermodynamics of liquid mixtures. New expression for the excess Gibbs energy of partly or completely miscible systems. AIChE J. **21**, 116–128 (1975)
13. Helgeson, H.C., Kirkham, D.H., Flowers, G.C.: Theoretical prediction of the thermodynamic behavior of aqueous electrolytes at high pressures and temperatures I. Summary of the thermodynamic/electrostatic properties of the solvent. Am. J. Sci. **274**, 1089–1198 (1974). Theoretical prediction of the thermodynamic behavior of aqueous electrolytes at high pressures and temperatures. II. Debye–Hückel parameters for activity coefficients and relative partial molal properties. Ibid. **274**, 1199–1261 (1974). Theoretical prediction of the thermodynamic behavior of aqueous electrolytes at high pressures and temperatures. III. Equation of state for aqueous species at infinite dilution. Ibid. **276,** 97–240 (1976); Theoretical prediction of the thermodynamic behavior of aqueous electrolytes at high pressures and temperatures. IV. Calculation of activity coefficients, osmotic coefficients, and apparent molal and standard and relative partial molal properties to 5 kb and 600 °C. Ibid. **281**, 1241–1516 (1981)
14. Tanger, J.C., Helgeson, H.C.: Calculation of the thermodynamic and transport properties of aqueous species at high pressures and temperatures: Revised equations of state for the standard partial molal properties of ions and electrolytes. Am. J. Sci. **288**, 19–98 (1988)
15. Shock, E.L., Helgeson, H.C., Sverjensky, D.A.: Calculation of the thermodynamic and transport properties of aqueous species at high pressures and temperatures: Standard partial molal properties of inorganic neutral species. Geochim. Cosmochim. Acta **53**, 2157–2183 (1989)
16. Shock, E.L., Helgeson, H.C.: Calculation of the thermodynamic and transport properties of aqueous species at high pressures and temperatures: Correlation algorithms for ionic species and equation of state predictions to 5 kb and 1000 °C. Geochim. Cosmochim. Acta **52**, 2009–2036 (1988). Calculation of the thermodynamic and transport properties of aqueous species at high pressures and temperatures: Standard partial molal properties of organic species. Ibid. **54**, 915–943 (1990)
17. Shock, E.L., Sassani, D.C., Willis, M., Sverjensky, D.A.: Inorganic species in geologic fluids: Correlations among standard molal thermodynamic properties of aqueous ions and hydroxide ions. Geochim. Cosmochim. Acta **61**, 907–950 (1997)
18. Sverjensky, D.A., Shock, E.L., Helgeson, H.C.: Prediction of the thermodynamic properties of aqueous metal complexes to 1000 °C and 5 kb. Geochim. Cosmochim. Acta **61**, 1359–1412 (1997)
19. Linke, W.F., Seidell, A.S.: Solubilities of Inorganic and Metal Organic Compounds K-Z, vol. 2, 4th edn. American Chemical Society, Washington (1965)
20. Vyazova, V.V., Pelsha, A.D.: Handbook of Experimental Solubility Data for Binary Aqueous and Nonaqueous Systems Containing Group I Elements, vol. 3. Khimia, Leningrad (1961)
21. Cohen-Adad, R., Lorimer, J.W.: Alkali Metal and Ammonium Chlorides in Water and Heavy Water (Binary Systems). Solubility Data Series, vol. 47. Pergamon, Oxford (1991)

22. Rard, J.A.: Results from boiling temperature measurements for saturated solutions in the systems $NaCl + Ca(NO_3)_2 + H_2O$, $NaNO_3 + KNO_3 + H_2O$, and $NaCl + KNO_3 + H_2O$, and dry out temperatures for $NaCl + NaNO_3 + KNO_3 + Ca(NO_3)_2 + H_2O$, Report UCRL-TR-217415, Lawrence Livermore National Laboratory (2005)
23. Rard, J.A.: Results from boiling temperature measurements for saturated solutions in the systems $NaCl + KNO_3 + H_2O$, $NaNO_3 + KNO_3 + H_2O$, and $NaCl + NaNO_3 + KNO_3 + H_2O$, Report UCRL-TR-207054, Lawrence Livermore National Laboratory (2004)
24. Archer, D.G.: Thermodynamic properties of the $NaCl + H_2O$ System II. Thermodynamic properties of NaCl(aq), $NaCl{\cdot}2H_2O$(cr), and phase equilibria. J. Phys. Chem. Ref. Data **21**, 793–829 (1992)
25. Archer, D.G.: Thermodynamic properties of the $NaCl + H_2O$ System I. Thermodynamic properties of NaCl(cr). J. Phys. Chem. Ref. Data **21**, 1–21 (1992)
26. Sohnel, O., Novotny, P.: Densities of Aqueous Solutions of Inorganic Substances. Elsevier, Amsterdam (1985)
27. Zaytsev, I.D., Aseyev, G.G.: Properties of Aqueous Solutions of Electrolytes. CRC Press, Boca Raton (1992)
28. Holmes, F.G., Baes Jr., C.F., Mesmer, R.E.: Isopiestic studies of aqueous solutions at elevated temperatures I. KCl, $CaCl_2$, and $MgCl_2$. J. Chem. Thermodyn. **10**, 983–996 (1978)
29. Ellis, A.J.: Partial molal volumes of alkali chlorides in aqueous solution to 200 °C. J. Chem. Soc. A Inorg. Phys. Theor. 1579–1584 (1966)
30. Khaibullin, I.Kh., Borisov, N.M.: Experimental investigation of the thermal properties of aqueous and vapor solutions of sodium and potassium chlorides at phase equilibrium high temperature. High Temp. **4**, 489–494 (1966)
31. Mayrath, J.E., Wood, R.H.: Enthalpy of dilution of aqueous solutions of LiCl, NaBr, NaI, KCl, KBr, and CsCl at about 373, 423, and 473 K. J. Chem. Thermodyn. **14**, 563–576 (1982)
32. Holmes, H.F., Mesmer, R.E.: Thermodynamic properties of aqueous solutions of the alkali metal chlorides to 250 °C. J. Phys. Chem. **87**, 1242–1255 (1983)
33. Pabalan, R.T., Pitzer, K.S.: Apparent molar heat capacity and other thermodynamic properties of aqueous KCl solutions to high temperatures and pressures. J. Chem. Eng. Data **33**, 354–362 (1988)
34. Gillespie, S.E., Chen, X., Oscarson, J.L., Izatt, R.M.: Enthalpies of dilution of aqueous solutions of LiCl, KCl, and CsCl at 300, 325 and 350 °C. J. Solution Chem. **26**, 47–61 (1997)
35. Archer, D.G.: Thermodynamic properties of the $KCl + H_2O$ systems. J. Phys. Chem. Ref. Data **28**, 1–17 (1999)
36. Pelsha, A.D.: Handbook of Experimental Data of Salt Solubilities, Binary Systems, Elements IIA, vol. 4. Khimiya, Leningrad (1963)
37. Sako, T., Hakuta, T., Yoshitome, H.J.: Vapor pressures of binary (H_2O–HCl, –$MgCl_2$, and –$CaCl_2$) and Ternary (H_2O–$MgCl_2$–$CaCl_2$) aqueous solutions. J. Chem. Eng. Data **30**, 224–228 (1985)
38. Urusova, M.A., Valyashko, V.M.: The vapour pressure and the activity of water in concentrated aqueous solutions containing the chlorides of alkali metals (Li, K, Cs) and alkaline earth metals (Mg, Ca) at increased temperature. Russ. J. Inorg. Chem. **32**, 23–26 (1987)
39. Oscarson, J.L., Gillespie, S.E., Chen, X., Schuck, P.C., Izatt, R.M.: Enthalpies of dilution of aqueous solutions of HCl, $MgCl_2$, $CaCl_2$, and $BaCl_2$ at 300, 325, and 350 °C. J. Solution Chem. **30**, 31–53 (2001)
40. Wagman, D.D., Evans, W.H., Parker, V.B., Schumm, R.H., Halow, I., Bailey, S.M., Churney, K.L., Nuttall, R.L.: The NBS tables of chemical thermodynamic properties, selected values for inorganic and C1 and C2 organic substances in SI units. J. Phys. Chem. Ref. Data **11**, 1–392 (1982)
41. Robinson, R.A., Stokes, R.H.: Electrolyte Solutions, 2nd edn. Butterworths, London (1970)
42. Rodebush, W.H.: The freezing points of concentrated solutions and the free energy of solution of salts. J. Am. Chem. Soc. **40**, 1204–1213 (1918)
43. Ha, Z., Chan, C.K.: The water activities of $MgCl_2$, $Mg(NO_3)_2$, $MgSO_4$, and their mixtures. Aerosol Sci. Technol. **31**, 154–169 (1999)
44. Platford, R.E.: Isopiestic measurements on the system water–sodium chloride–magnesium chloride at 25 °C. J. Phys. Chem. **72**, 4053–4057 (1968)
45. Wu, Y.C., Rush, R.M., Scatchard, G.: Osmotic and activity coefficients for binary mixtures of sodium chloride, sodium sulfate, magnesium sulfate, and magnesium chloride in water at 25 °C. I. Isopiestic measurements on the four systems with common ions. J. Phys. Chem. **72**, 4048–4053 (1968)
46. Gibbard Jr., H.F., Gossmann, A.F.: Freezing points of electrolyte mixtures I. Mixtures of sodium chloride and magnesium chloride in water. J. Solution Chem. **3**, 385–393 (1974)
47. Rard, J.A., Miller, D.G.: Isopiestic determination of the osmotic and activity coefficients of aqueous mixtures of NaCl and $MgCl_2$ at 25 °C. J. Chem. Eng. Data **32**, 85–92 (1987)
48. Padova, J., Saad, D.: Thermodynamics of mixed electrolyte solutions. VIII. An isopiestic study of the ternary system: KCl–$MgCl_2$–H_2O at 25 °C. J. Solution Chem. **6**, 57–51 (1977)

49. Kuschell, F., Seidel, J.: Osmotic and activity coefficients of aqueous K_2SO_4–$MgSO_4$ and KCl–$MgCl_2$ at 25 °C. J. Chem. Eng. Data **30**, 440–445 (1985)
50. Prutton, C.F., Tower, O.F.: The system calcium chloride–magnesium chloride–water at 0, −15 and −30 °C. J. Am. Chem. Soc. **54**, 3040–3047 (1932)
51. Robinson, R.A., Bower, V.E.: Properties of aqueous mixtures of pure salts. Thermodynamics of the ternary system: Water–sodium chloride–calcium chloride at 25 °C. J. Res. Nat. Bur. Stand. A **70**, 304–311 (1966)
52. Saad, D., Padova, J., Marcus, Y.: Thermodynamics of mixed electrolyte solutions. VI. An isopiestic study of a pseudo-ternary system: NaCl–KCl–$MgCl_2$–H_2O at 25 °C. J. Solution Chem. **4**, 983–933 (1975)
53. Washburn, E.W.: International Critical Tables of Numerical Data, Physics, Chemistry and Technology, vol. 3. McGraw-Hill, New York (1928)
54. Washburn, E.W.: International Critical Tables of Numerical Data, Physics, Chemistry and Technology, vol. 4. McGraw-Hill, New York (1928)
55. Fricke, R.: Zum thermodynamischen Verhalten konzentrierter Lösungen. Z. Elektrochem. **35**, 631–640 (1929)
56. Lange, E., Streeck, H.: Verdünnungswärmen einiger zwei-ein-wertiger Salze in grosser Verdünnung bei 25 °C. I. $MgCl_2$, $CaCl_2$, $SrCl_2$, $BaCl_2$ and $MgBr_2$, $CaBr_2$, $SrBr_2$, $BaBr_2$. Z. physik. Chem. **152**, 1–23 (1931)
57. Robinson, R.A., Stokes, R.H.: A thermodynamic study of bivalent metal halides in aqueous solution. Part I. The activity coefficients of magnesium halides at 25 °C. Trans. Faraday Soc. **6**, 733–734 (1940)
58. Stokes, R.H.: A thermodynamic study of bivalent metal halides in aqueous solution. Part XIV. Concentrated solutions of magnesium chloride at 25 °C. Trans. Faraday Soc. **41**, 642–645 (1945)
59. Eigen, V.M., Wicke, E.: Ionenhydratation und spezifische Wärme wäßriger Elektrolytlösungen. Z. Elektrochem. **55**, 354–363 (1951)
60. Dunn, L.A.: Apparent molar volumes of electrolytes. Part 1. Some 1-1, 1-2, 2-1, 3-1 electrolytes in aqueous solution at 25 °C. Trans. Faraday Soc. **62**, 2348–2353 (1966)
61. Ellis, A.J.: Partial molal volumes of $MgCl_2$, $CaCl_2$, $SrCl_2$, and $BaCl_2$ in aqueous solution to 200 °C. J. Chem. Soc. A Inorg. Phys. Theor., 660–664 (1967)
62. Lindsay Jr., W.T., Liu, C.T.: Vapor pressure lowering of aqueous solutions at elevated temperatures. OSW R&D Rep. **347**, 133–138 (1968)
63. Fedyainov, N.W., Vasilev, V.A., Karapetyants, M.Kh.: Specific heat of two- and three- component aqueous solutions of beryllium subgroup metal chlorides at 25 °C. Russ. J. Phys. Chem. **44**, 1026–1027 (1970)
64. Frolov, Y.G., Nikolaev, V.P., Karapetyants, M.Kh., Vlasenko, K.K.: Excess thermodynamic functions of mixing of aqueous isopiestic electrolyte solutions without common ions. Russ. J. Phys. Chem. **45**, 1054–1055 (1971)
65. Liu, C.T., Lindsay Jr., W.T.: Thermodynamic properties of aqueous solutions at high temperatures. OSW R&D Rep. **722**, 59–64 (1971)
66. Likke, S., Bromley, L.A.: Heat capacities of aqueous NaCl, KCl, $MgCl_2$, $MgSO_4$, and Na_2SO_4 solutions between 80 and 200 °C. J. Chem. Eng. Data **18**, 189–195 (1973)
67. Vasilev, Y.A., Fedyainov, N.W., Kurenkov, V.V.: Specific heats and specific volumes of isopiestic aqueous solutions of beryllium subgroup metal chlorides. Russ. J. Phys. Chem. **47**, 1570–1573 (1973)
68. Perron, G., Desnoyers, J.E., Millero, F.J.: Apparent molal volumes and heat capacities of alkaline earth chlorides in water at 25 °C. Can. J. Chem. **52**, 3738–3741 (1974)
69. Leung, W.H., Millero, F.J.: The enthalpy of formation of magnesium sulfate ion pairs. J. Solution Chem. **4**, 145–159 (1975)
70. Snipes, H.P., Manly, C., Enson, D.D.: Heats of dilution of aqueous electrolytes: Temperature dependence. J. Chem. Eng. Data **20**, 287–291 (1975)
71. Chen, C.-T., Emmet, R.T., Millero, F.J.: The apparent molal volumes of aqueous solutions of NaCl, KCl, $MgCl_2$, Na_2SO_4, and $MgSO_4$ from 0 to 1000 bars at 0, 25, and 50 °C. J. Chem. Eng. Data **22**, 201–207 (1977)
72. Goldberg, R.N., Nuttall, R.L.: Evaluated activity and osmotic coefficients for aqueous solutions: The alkaline earth metal halides. J. Phys. Chem. Ref. Data **7**, 263–310 (1978)
73. Clynne, M.A., Potter II, R.W.: Solubility of some alkali and alkaline earth chlorides in water at moderate temperatures. J. Chem. Eng. Data **24**, 338–340 (1979)
74. Phang, S., Stokes, R.H.: Density viscosity, conductance, and transference number of concentrated aqueous magnesium chloride at 25 °C. J. Solution Chem. **9**, 497–505 (1980)
75. Perron, G., Roux, A., Desnoyers, J.E.: Heat capacities and volumes of NaCl, $MgCl_2$, $CaCl_2$, and $NiCl_2$ up to 6 molal in water. Can. J. Chem. **59**, 3049–3054 (1981)

76. Rard, J.A., Miller, D.G.: Isopiestic determination of the osmotic and activity coefficients of aqueous $MgCl_2$ solutions at 25 °C. J. Chem. Eng. Data **26**, 38–43 (1981)
77. Matuzenko, M.Yu., Puchkov, D.V., Zarembo, V.I.: Collected Abstracts: 9th All-Union Conf. on Calorimetry and Chemical Thermodynamics, Tbilisi, pp. 157–159 (1982)
78. Surdo, A.L., Alzola, E.M., Millero, F.J.: The PVT properties of concentrated aqueous electrolytes. I. Densities and apparent molar volumes of NaCl, Na_2SO_4, $MgCl_2$, and $MgSO_4$ solutions from 0.1 mol/kg to saturation and from 273.15 to 323.15 K. J. Chem. Thermodyn. **14**, 649–662 (1982)
79. Mayrath, J.E., Wood, R.H.: Enthalpy of dilution of aqueous solutions of Na_2SO_4, K_2SO_4, and $MgSO_4$ at 373.15 and 423.65 K and of $MgCl_2$ at 373.15, 423.65, and 472.95 K. J. Chem. Eng. Data **28**, 56–59 (1983)
80. Romankiw, L.A., Chou, I.-M.: Densities of aqueous NaCl, KCl, $MgCl_2$, and $CaCl_2$ binary solutions in the concentration range 0.5–6.1 *m* at 25, 30, 35, 40, and 45 °C. J. Chem. Eng. Data **28**, 300–305 (1983)
81. Urusova, M.A., Valyashko, V.M.: Solubility, vapour pressure, and thermodynamic properties of solutions in the $MgCl_2$–H_2O system at 300–350 °C. Russ. J. Inorg. Chem. **28**, 1045–1048 (1983)
82. Gates, J.A., Wood, R.H.: Densities of aqueous solutions of NaCl, $MgCl_2$, KCl, NaBr, LiCl, and $CaCl_2$ from 0.05 to 5.0 mol/kg and 0.1013 to 40 MPa at 298.15 K. J. Chem. Eng. Data **30**, 44–49 (1985)
83. Juillard, J., Tissier, C., Barczynska, J., Mokrzan, J., Taniewska-Osinska, S.: Solute–solvent interactions in water-*t*-butyl alcohol mixtures. Part 14. ΔG, ΔH and ΔS of transfer for alkaline earth metal cations. J. Chem. Soc. Faraday Trans. I **81**, 3081–3090 (1985)
84. Connaughton, L.M., Hershey, J.P., Millero, F.J.: PVT properties of concentrated aqueous electrolytes: V. Densities and apparent molal volumes of the four major sea salts from dilute solution to saturation and from 0 to 100 °C. J. Solution Chem. **15**, 989–1002 (1986)
85. Emons, H.H., Voigt, W., Wollny, W.F.: Dampfdruckmessungen am System Magnesiumchlorid–Wasser. Z. physik. Chem. Leipzig **267**, 1–8 (1986)
86. Fanghanel, T., Kravchuk, K., Voigt, W., Emons, H.H.: Solid–liquid phase equilibria in the system KCl–$MgCl_2$–H_2O at elevated temperatures. I. The binary system $MgCl_2$–H_2O at 130–250 °C. Z. Anorg. Allgem. Chem. **547**, 21–26 (1987)
87. Saluja, P.P.S., LeBlanc, J.C.: Apparent molar heat capacities and volumes of aqueous solutions of $MgCl_2$, $CaCl_2$, and $SrCl_2$ at elevated temperatures. J. Chem. Eng. Data **32**, 72–76 (1987)
88. White, D.E., Gates, J.A., Tillet, D.M., Wood, R.H.: Heat capacity of aqueous $CaCl_2$ from 306 to 603 K at 17.5 MPa. J. Chem. Eng. Data **33**, 485–490 (1988)
89. Fanghanel, T., Grjotheim, K.: Thermodynamics of aqueous reciprocal salt systems. III. Isopiestic determination of osmotic and activity coefficients of aqueous $MgCl_2$, $MgBr_2$, KCl and KBr at 100.3 °C. Acta Chem. Scand. **44**, 892–895 (1990)
90. Pepinov, R.I., Labkova, N.V., Zokhraggekova, G.Y.: Density of water solutions of magnesium-chloride and magnesium-sulfate at high-temperatures and pressures. High Temp. **30**, 66–70 (1992)
91. Jahn, H., Wolf, G.: The enthalpy of solution of $MgCl_2$ and $MgCl_2{\cdot}6H_2O$ in water at 25 °C. I. The integral molar enthalpy of solution. J. Solution Chem. **22**, 893–994 (1993)
92. Saluja, P.P.S., Jobe, D.J., LeBlanc, J.C., Lemire, R.J.: Apparent molar heat capacities and volumes of mixed electrolytes: [NaCl(aq) + $CaCl_2$(aq)], [NaCl(aq) + $MgCl_2$(aq)], and [$CaCl_2$(aq) + $MgCl_2$(aq)]. J. Chem. Eng. Data **40**, 398–406 (1995)
93. Holmes, H.F., Mesmer, R.E.: Aqueous solutions of the alkaline earth metal chlorides at elevated temperatures. Isopiestic molalities and thermodynamic properties. J. Chem. Thermodyn. **28**, 1325–1358 (1996)
94. Obsil, M., Majer, V., Hefter, G.T., Hynek, V.: Volumes of $MgCl_2$(aq) at temperatures from 298 K to 623 K and pressures up to 30 MPa. J. Chem. Thermodyn. **29**, 575–593 (1997)
95. Wang, P., Oakes, C.S., Pitzer, K.S.: Thermodynamics of aqueous mixtures of magnesium chloride with sodium chloride from 298.15 to 573.15 K. New measurements of the enthalpies of mixing and of dilution. J. Chem. Eng. Data **42**, 1101–1110 (1997)
96. Call, T.G., Ballerat-Busserolles, K., Origlia, M.L., Ford, T.D., Woolley, E.M.: Apparent molar volumes and heat capacities of aqueous magnesium chloride and cadmium chloride at temperatures from 278.15 K to 393.15 K at the pressure 0.35 MPa: A comparison of ion–ion interactions. J. Chem. Thermodyn. **32**, 1525–1538 (2000)
97. Linke, W.F., Seidell, A.S.: Solubilities of Inorganic and Metal-Organic Compounds A-Ir, vol. 1, 4th edn. American Chemical Society, Washington (1958)
98. Oakes, C.S., Bodnar, R.J., Simonson, J.M.: The system NaCl–$CaCl_2$–H_2O: I. The ice liquidus at 1 atm total pressure. Geochim. Cosmochim. Acta **54**, 603–610 (1990)
99. Zarembo, V.I., Livov, S.N., Matuzenko, M.Yu.: Saturated vapor pressure of water and activity coefficients of calcium chloride in the $CaCl_2$–H_2O system at 423–623 K. Geochem. Int. **17**, 159–162 (1980)
100. Ketsko, V.A., Urusova, M.A., Valyashko, W.M.: Solubility and vapour pressure of solutions in the $CaCl_2$–H_2O system at 250–400 °C. Russ. J. Inorg. Chem. **29**, 1398–1399 (1984)

101. Wood, S.A., Crerar, D.A., Brantley, S.L., Borcsik, M.: Mean molal stoichiometric activity coefficients of alkali halides and related electrolytes in hydrothermal solutions. Am. J. Sci. **284**, 668–705 (1984)
102. Ananthaswamy, J., Atkinson, G.J.: Thermodynamics of concentrated electrolyte mixtures. 5. A review of the thermodynamic properties of aqueous calcium chloride in the temperature range 273.25–373.15 K. J. Chem. Eng. Data **30**, 120–128 (1985)
103. Simonson, J.M., Busey, R.H., Mesmer, R.E.: Enthalpies of dilution of aqueous calcium chloride to low molalities at high temperatures. J. Phys. Chem. **89**, 557–560 (1985)
104. Garvin, D., Parker, V.B., White, H.J.: CODATA Thermodynamic Tables, Selections for Some Compounds of Calcium and Related Mixtures: A Prototype Set of Tables. Hemisphere Publishing, Washington (1987)
105. White, D.E., Doberstein, A.L., Gates, J.A., Tillet, D.M., Wood, R.H.: Heat capacity of aqueous $CaCl_2$ from 306 to 603 K at 17.5 MPa. J. Chem. Thermodyn. **19**, 251–259 (1987)
106. Holmes, H.F., Busey, R.H., Simonson, J.M., Mesmer, R.E.: $CaCl_2$(aq) at elevated temperatures. Enthalpies of dilution, isopiestic molalities, and thermodynamic properties. J. Chem. Thermodyn. **26**, 271–298 (1994)
107. Pitzer, K.S., Oakes, C.S.: Thermodynamics of calcium chloride in concentrated aqueous solutions and in crystals. J. Chem. Eng. Data **39**, 553–559 (1994)
108. Oakes, C.S., Simonson, J.M., Bodnar, R.J.: Apparent molar volumes of aqueous calcium chloride to 250 °C, 400 bars, and from molalities of 0.242 to 6.150. J. Solution Chem. **24**, 897–916 (1995)
109. Hoffmann, F.P., Voigt, W.: Vapor pressure of highly concentrated aqueous calcium chloride solutions (3.8–25 mol/kg) at temperatures from 373 to 523 K. Int. Elect. J. Phys Chem. Data **2**, 31–36 (1996)
110. Rard, J.A., Clegg, S.L.: Critical evaluation of the thermodynamic properties of aqueous calcium chloride. 1. Osmotic and activity coefficients of 0–10.77 $mol \cdot kg^{-1}$ aqueous calcium chloride solutions at 298.15 K and correlation with extended Pitzer ion-interaction models. J. Chem. Eng. Data **42**, 819–849 (1997)
111. Oakes, C.S., Pitzer, K.S., Sterner, S.M.: The system NaCl–$CaCl_2$–H_2O: Part 3. Heats of dilution and mixing at 373 to 573 K and 21.5 MPa using a new high temperature, flow-through calorimeter. Geochim. Cosmochim. Acta **62**, 1133–1146 (1998)
112. Guendouzi, M.E., Marouani, M.: Water activities and osmotic and activity coefficients of aqueous solutions of nitrates at 25 °C by the hygrometric method. J. Solution Chem. **32**, 535–546 (2003)
113. Bezboruah, C.P., Covington, A.K., Robinson, R.A.: Excess Gibbs energies of aqueous mixtures of alkali metal chlorides and nitrates. J. Chem. Thermodyn. **2**, 431–437 (1970)
114. Kirgintsev, A.N., Lukyanov, A.V.: Issledovanie troinykh rastvorov izopesticheskim metodom. III. Troinye rastvory NaCl–$NaNO_3$–H_2O, NaCl–NaBr–H_2O, NH_4Cl–NH_4Br–H_2O. Russ. J. Phys. Chem. **39**, 653–655 (1965)
115. Lincoln, A.T., Klein, D.: The vapor pressure of aqueous nitrate solutions. J. Phys. Chem. **11**, 318–348 (1907)
116. Robinson, R.A.: The activity coefficients of alkali nitrates, acetates and *p*-toluenesulfonates in aqueous solution from vapor pressure measurements. J. Am. Chem. Soc. **57**, 1165–1168 (1935)
117. Kangro, W., Groeneveld, A.: Concentrated aqueous solutions. I. Z. physik. Chem. N.F. **32**, 110–126 (1962)
118. Shpigel, L.P., Mishchenko, K.P.: Activities and rational activity coefficients of water in potassium nitrate and sodium nitrate solutions at 1, 25, 50, and 75 °C over a wide concentration range. Russ. J. Appl. Chem. **40**, 659–661 (1967)
119. Puchkove, L.V., Matveeva, R.P., Baranova, T.L.: Specific heats of aqueous solutions of sodium and potassium nitrates at temperatures in the range 25–340 °C. Russ. J. Appl. Chem. **46**, 460–462 (1973)
120. Egorov, V.Ya., Zarembo, V.I., Soboleva, N.G., Puchkov, L.V.: Activity of water and activity coefficients of dissolved electrolytes in aqueous solutions of alkali metal nitrates at temperatures of 423–623 K. Russ. J. Appl. Chem. **54**, 1031–1034 (1981)
121. Azizov, N.D., Akhundov, T.S.: Experimental study of solvent vapor pressure and calculation of thermodynamic properties for $NaNO_3$–H_2O and KNO_3–H_2O mixtures. Russ. J. Inorg. Chem. **43**, 1600–1603 (1998)
122. Kirgintsev, A.N., Lukyanov, A.V.: Isopiestic investigation of ternary solutions. V. Ternary $NaNO_3$–$Ca(NO_3)_2$–H_2O, $NaNO_3$–$La(NO_3)_3$–H_2O, $NaNO_3$–$Th(NO_3)_4$–H_2O, NaCl–$CaCl_2$–H_2O, NaCl–$LaCl_3$–H_2O and NaCl–$ThCl_4$–H_2O solutions at 25 °C. Russ. J. Phys. Chem. **39**, 389–391 (1965)
123. Kirgintsev, A.N., Lukyanov, A.V.: Issledovanie troinykh rastvorov izopesticheskim metodom. III. Troinye rastvory NaCl–$NaNO_3$–H_2O, NaCl–NaBr–H_2O, NH_4Cl–NH_4Br–H_2O. Russ. J. Phys. Chem. **38**, 867–869 (1964)
124. Berkeley, E.: On some physical constants of saturated solutions. Philos. Trans. Roy. Soc. London **203**, 189–215 (1904)

125. Chretian, A.: Etude du systeme quaternaire eau, nitrate de sodium, chlorure de sodium, sulfate de sodium. Annal. Chim. Paris **12**, 9–155 (1929)
126. Kracek, F.C.: Gradual transition in sodium nitrate. I. Physicochemical criteria of the transition. J. Am. Chem. Soc. **53**, 2609–2624 (1931)
127. Pearce, J.N., Hopson, H.: The vapor pressures of aqueous solutions of sodium nitrate and potassium. Thiocyanate. J. Phys. Chem. **41**, 535–538 (1937)
128. Puchkov, L.V., Matashkin, V.G.: Densities of $LiNO_3$–H_2O and $NaNO_3$–H_2O solutions at temperatures in the range 25–300 °C. Russ. J. Appl. Chem. **43**, 1864–1867 (1970)
129. Greyson, J., Snell, H.: Heat of transfer between heavy and normal water for some inorganic acid salts. J. Chem. Eng. Data **16**, 73–74 (1971)
130. Shenkin, Ya.S., Ruchnova, S.A., Rodionova, N.A.: Solubility isobars for the sodium nitrite–sodium nitrate–water system. Russ. J. Inorg. Chem. **18**, 123–124 (1973)
131. Natarajan, T.S., Srinivasan, D.: Effect of sodium nitrate on the vapor–liquid equilibria of the methanol–water system. J. Chem. Eng. Data **25**, 281–221 (1980)
132. Wu, Y.C., Hamer, W.J.: Comments: revised values of the osmotic coefficients and mean activity coefficients of sodium nitrate in water at 25 °C. J. Phys. Chem. Ref. Data **9**, 513–518 (1980)
133. Voigt, W., Dittrich, A., Haugsdal, B., Grjotheim, K.: Thermodynamics of aqueous reciprocal salt systems. II. Isopiestic determination of the osmotic and activity coefficients in $LiNO_3$–NaBr–H_2O and LiBr–$NaNO_3$–H_2O at 100.3 °C. Acta Chem. Scand. **44**, 12–17 (1990)
134. Apelblat, A.: The vapour pressures of saturated aqueous lithium chloride, sodium bromide, sodium nitrate, ammonium nitrate, and ammonium chloride at temperatures from 283 K to 313 K. J. Chem. Thermodyn. **25**, 63–71 (1993)
135. Bozmann, E., Richter, J., Stark, A.: Experimental results and aspects of analytical treatment of vapour pressure measurements in hydrated melts at elevated temperatures. Ber. Bunsenges. Phys. Chem. **97**, 240–245 (1993)
136. Tang, I.N., Munkelwitz, H.R.: Water activities, densities, and refractive indices of aqueous sulfates and sodium nitrate droplets of atmospheric importance. J. Geophys. Res. **99**, 18801–18808 (1994)
137. Pena, M.P., Vercher, E., Martinez-Andreu, A.J.: Vapor–liquid equilibrium for ethanol + water + sodium nitrate. J. Chem. Eng. Data **41**, 1097–1100 (1996)
138. Archer, D.G.: Thermodynamic properties of the $NaNO_3 + H_2O$ system. J. Phys. Chem. Ref. Data **29**, 1141–1156 (2000)
139. Carter, R.W., Archer, D.G.: Heat capacity of $NaNO_3$(aq) in stable and supercooled states. Ion association in the supercooled solution. Phys. Chem. Chem. Phys. **2**, 5138–5145 (2000)
140. Guendouzi, M.E., Dinane, A.J.: Determination of water activities, osmotic and activity coefficients in aqueous solutions using the hygrometric method. J. Chem. Thermodyn. **32**, 297–310 (2000)
141. Apelblat, A., Korin, E.: Vapor pressures of saturated aqueous solutions of ammonium iodide, potassium iodide, potassium nitrate, strontium chloride, lithium sulphate, sodium thiosulphate, magnesium nitrate, and uranyl nitrate from $T = (278 \text{ to } 323)$ K. J. Chem. Thermodyn. **30**, 459–471 (1998)
142. Rodnyanskii, I.M., Korobkov, V.I., Galinker, I.S.: Specific volumes of aqueous electrolyte solutions at high temperatures. Russ. J. Phys. Chem. **36**, 1192–1194 (1962)
143. Amdur, S.M., Padova, J.I., Schwarz, A.M.: Isopiestic study of the system potassium chloride–potassium nitrate–water at 25 °C. J. Chem. Eng. Data **15**, 417–418 (1970)
144. Fanghanel, T., Grjotheim, K., Voigt, W., Brendler, V.: Thermodynamics of aqueous reciprocal salt systems. VI. Isopiestic determination of osmotic coefficients in mixtures of chlorides, bromides and nitrates of lithium, sodium, potassium and cesium at 100.3 °C. Acta Chem. Scand. **46**, 423–431 (1992)
145. Parker, V.B.: Thermal properties of aqueous uni-univalent electrolytes. National Standard Ref. Data Series National Bureau of Standards, vol. 2 (1965)
146. Hamer, W.J., Wu, Y.-C.: Osmotic coefficients and mean activity coefficients of uni-univalent electrolytes in water at 25 °C. J. Phys. Chem. Ref. Data **1**, 1047–1099 (1972)
147. Petrov, G.I., Puchkov, L.V.: Adiabatic calorimeter for measuring specific heats of liquids in the temperature range from 0 to 100 °C. Russ. J. Appl. Chem. **46**, 2373–2375 (1973)
148. Simonson, J.M., Pitzer, K.S.: Thermodynamics of multicomponent, miscible, ionic systems: The system $LiNO_3$–KNO_3–H_2O. J. Phys. Chem. **90**, 3009–3013 (1986)
149. Barry, J.C., Richter, J., Stich, E.: Vapor pressures and ionic activity coefficients in the system $KNO_3 + H_2O$ from dilute solutions to fused salts at 425 K, 452 K, and 492 K. Ber. Bunsenges. Phys. Chem. **92**, 1118–1122 (1988)
150. Vercher, E., Pena, M.P., Martinez-Andreu, A.: Isobaric vapor–liquid equilibrium for ethanol + water + potassium nitrate. J. Chem. Eng. Data **41**, 66–69 (1996)
151. Ewing, W.W., Klinger, E., Brandner, J.D.: Studies on the vapor pressure–temperature relations and on the heats of hydration, solution and dilution of the binary system magnesium nitrate–water. J. Am. Chem. Soc. **56**, 1053–1057 (1934)

152. Robinson, R.A., Wilson, J.M., Ayling, H.S.: The activity coefficients of some bivalent metal nitrates in aqueous solution at 25 °C from isopiestic vapor pressure measurements. J. Am. Chem. Soc. **64**, 1469–1471 (1942)
153. Forsythe, W.E.: Smithsonian Phys. Tables, 9th edn., pp. 373–374. Smithsonian Institution Press, Washington (1954)
154. Jain, S.K.: Volumetric properties of some single molten hydrated salts. J. Chem. Eng. Data **22**, 383–385 (1977)
155. Sadowska, T., Libuś, W.: Thermodynamic properties and solution equilibria of aqueous bivalent transition metal nitrates and magnesium nitrate. J. Solution Chem. **11**, 457–468 (1982)
156. Jubin, R.T., Marley, J.L., Counce, R.M.: Density study of $Mg(NO_3)_2$–H_2O–HNO_3 solutions at different temperatures. J. Chem. Eng. Data **31**, 86–88 (1986)
157. Akhundov, T.S., Akhmedova, I.N., Iskenderov, A.I.: Thermal properties of aqueous solutions of magnesium nitrate in a wide range of pressures and temperatures. Izv. Vyss. Ucheb. Zaved. Neft. Gaz. **12**, 66–69 (1989)
158. Apelblat, A.: The vapor pressures of water over saturated aqueous solutions of barium chloride, magnesium nitrate, calcium nitrate, potassium carbonate, and zinc sulfate, at temperatures from 283 K to 313 K. J. Chem. Thermodyn. **24**, 619–626 (1992)
159. Todorovic, M., Ninkovic, R.: Osmotic and activity coefficients of $\{xMg(NO_3)_2 + (1-x)MgSO_4\}$(aq) at the temperature 298.15 K. J. Chem. Thermodyn. **27**, 369–375 (1995)
160. Todorovic, M., Ninkovic, R., Miladinovic, J.: Osmotic and activity coefficients of $\{yK_2SO_4 + (1-y)Mg(NO_3)_2\}$(aq) at the temperature 298.15 K. J. Chem. Thermodyn. **30**, 847–853 (1998)
161. Ewing, W.W.: Calcium nitrate. II. The vapor pressure–temperature relations of the binary system calcium nitrate–water. J. Am. Chem. Soc. **49**, 1963–1973 (1927)
162. Robinson, R.A.: The activity coefficient of calcium nitrate in aqueous solution at 25 °C from isopiestic vapor pressure measurements. J. Am. Chem. Soc. **62**, 3130–3131 (1940)
163. Stokes, R.H., Robinson, R.A.: Ionic hydration and activity in electrolyte solutions. J. Am. Chem. Soc. **70**, 1870–1878 (1948)
164. Oakes, C.S., Felmy, A.R., Sterner, S.M.: Thermodynamic properties of aqueous calcium nitrate $\{Ca(NO_3)_2\}$ to the temperature 373 K including new enthalpy of dilution. Data J. Chem. Thermodyn. **32**, 29–54 (2000)
165. Pelsha, A.D.: Handbook of Experimental Data for Salt Solubilities, Ternary Systems, vol. 1. Khimia, Leningrad (1973)
166. Clynne, M.A., Potter II, R.W., Haas Jr., J.L.: Solubility of NaCl in aqueous electrolyte solutions from 10 to 100 °C. J. Chem. Eng. Data **26**, 396–398 (1981)
167. Robinson, R.A., Bower, V.E.: An additivity rule for the vapor pressure lowering of aqueous solutions. J. Res. Nat. Bur. Stand. A **69**, 365–367 (1965)
168. Assarsson, G.O.: Equilibria in aqueous systems containing K^+, Na^+, Ca^{++}, Mg^{++} and Cl^-. II. The quaternary system $CaCl_2$–KCl–NaCl–H_2O. J. Am. Chem. Soc. **72**, 1437–1441 (1950)
169. Shiah, I.M., Tseng, H.C.: Experimental and theoretical determination of vapor pressures of NaCl–KCl, NaBr–KBr and NaCl–$CaCl_2$ aqueous solutions at 298 to 343 K. Fluid Phase Equilib. **124**, 235–249 (1996)
170. Holluta, J., Mautner, S.: Investigations of the solubility influence of strong electrolytes. I. The mutual solubility effect of alkali salts having a common ion. I. Z. physik. Chem. **127**, 455–475 (1927)
171. Blasdale, W.C.: Equilibria in solutions containing mixtures of salts III. The system, water and the chlorides and carbonates of sodium and potassium at 25 °C. IV. The system, water and the sulfates and carbonates of sodium and potassium at 25 °C. J. Am. Chem. Soc. **45**, 2935–2946 (1923)
172. Teeple, J.E.: The Industrial Development of Searles Lake Brines. Chem. Catalogue Company, New York (1929)
173. Cornec, E., Krombach, H.: Equilibria between water, potassium chloride and sodium chloride between −23° and +190°. Ann. Chim. Appl. **18**, 5–31 (1932)
174. Cornec, E., Krombach, H.: Equilibria between water, potassium chloride and sodium chloride between −23° and +190°. Compt. Rend. **194**, 714–716 (1932)
175. Erdos, E.: Solubility of electrolytes. I. Presentation and correlation of solubility data in multicomponent systems. Chem. Listy Vedu Prum. **51**, 1632–1640 (1957)
176. Brunisholz, G., Bodmer, M.: The system H^+–Na^+–K^+–Cl^-–PO_4^{3-}–H_2O. I. General observations and the ternary systems NaCl–KCl–H_2O, KCl–KH_2PO_4–H_2O, NaCl–NaH_2PO_4–H_2O, and NaH_2PO_4–KH_2PO_4–H_2O. Helv. Chim. Acta **46**, 2566–2574 (1963)
177. Holmes, H.F., Baes Jr., C.F., Mesmer, R.E.: Isopiestic studies of aqueous solutions at elevated temperatures II. NaCl + KCl mixtures. J. Chem. Thermodyn. **11**, 1035–1050 (1979)
178. Sterner, S.M., Hall, D.L., Bodnar, R.J.: Synthetic fluid inclusions: V. Solubility relations in the system NaCl–KCl–H_2O under vapor–saturated conditions. Geochim. Cosmochim. Acta **52**, 989–1005 (1988)

179. Flesia, M.A., DeChialvo, M.R.G., Chialvo, A.C.: Isopiestic determination of osmotic coefficients and evaluation of activity coefficients of aqueous mixtures of sodium and potassium chloride at 45 °C. Fluid Phase Equilib. **131**, 189–196 (1997)
180. Keitel, H.: Rate of dissolution and displacement of sylvine and rock salt from natural sylvinite and "hard salt". Mitteil. Kali-Forschungs-Anstalt, 95–127 (1922)
181. Akhumov, E.I., Vasiliev, B.B.: Izvestiia Sektora Fiz. Khim. Analiza Inst. Obsh. Neorgan. Khim. Akad. Nauk SSSR **9**, 308 (1936), cited in: Ref. [294], p. 108
182. d'Ans, J., Sypiena, G.: Solubilities in the system $KCl–MgCl_2–H_2O$ and $NaCl–MgCl_2–H_2O$ at temperatures up to about 200°. Kali **36**, 89–95 (1942)
183. Majima, K., Tejima, M., Oka, S.: Natural gas brine. IV. Phase equilibriums in ternary systems $MgCl_2–CaCl_2–H_2O$ and $NaCl–MgCl_2–H_2O$ and a quaternary system $NaCl–MgCl_2–CaCl_2–H_2O$ at 50°. Nippon Kaisui Gakkaishi **23**, 113–117 (1969)
184. Sieverts, A., Muller, E.L.: Das reziproke Salzpaar $MgCl_2$, $Na_2(NO_3)_2$, H_2O. II. Z. Anorg. Allgem. Chem. **200**, 305–320 (1931)
185. Meyer, T.A., Prutton, C.F., Lightfoot, W.J.: Equilibria in saturated solutions. V. The quinary system $CaCl_2–MgCl_2–KCl–NaCl–H_2O$ at 35 °C. J. Am. Chem. Soc. **71**, 1236–1237 (1949)
186. Leimbach, G.: Beitrag zur Kenntnis der ozeanischen Salzablagerungen. Kali **1**, 8–13 (1926)
187. van't Hoff, J.H.: Zur Bildung der ozeanischen Salzablagerungen. Z. Anorg. Chem. **47**, 244–280 (1905)
188. van't Hoff, J.H., Dawson, H.M.: Schmelzpunktserniedrigung des Magnesiumchlorids durch Zusatz von Fremdkörpern. Z. Physik. Chem. **22**, 598–608 (1897)
189. van't Hoff, J.H., Sachs, H., Biach, O.: Untersuchungen über die Bildungsverhältnisse der ozeanischen Salzablagerungen. XXXV. Die Zusammensetzung der konstanten Lösungen bei 83°. Sitz. Konig. Preuss. Ak., 576–586 (1904)
190. d'Ans, J.: Researches on the salt systems of oceanic salt deposits. Kali **9**, 148–154 (1915)
191. Maeda, T.: Salt manufacturing processes. J. Chem. Ind. Japan **23**, 1129–1146 (1920)
192. Takegami, S.: Reciprocal salt pairs: $Na_2Cl_2 + MgSO_4 \rightarrow Na_2SO_4 + MgCl_2$ at 25°. Memoirs Coll. Sci. Kyoto Imp. University **4**, 317–342 (1921)
193. Keitel, H., Gerlach: The systems $KCl–MgCl_2–H_2O$ and $NaCl–MgCl_2–H_2O$. Kali **17**, 248–251, 261–265 (1923)
194. Kurnakow, N.S., Zemcuzny, S.F.: Die Gleichgewichte des reziproken Systems Natriumchlorid–Magnesiumsulfat mit Berücksichtigung der naturlichen Salzsolen. Z. Anorg. Allgem. Chem. **140**, 149–182 (1924)
195. Leimbach, G., Pfeiffenberger, A.: Quaternary system: sodium nitrate–sodium sulfate–magnesium chloride–water from 0°to 100°. Caliche **11**, 61–85 (1929)
196. Bergman, A.G., Koloskaova, Z.A., Dombrovskaya, N.S.: Za nedra Volgo Prikaspiya **2**, 312–313 (1937), cited in: Ref. [165], p. 290
197. Klementiev, V.: Tr. Vses. Alyumin. Magniev. Inst. **14**, 5–12 (1937), cited in: Ref. [165] p. 290
198. Nikolaev, V.I., Burovaya, E.E.: Surface tension and viscosity in the reciprocal system sodium chloride–magnesium sulfate. Ann. Sect. Anal. Phys.-Chim., Inst. Chim. Gen. (U.S.S.R.) **10**, 245–258 (1938)
199. Rode, T.V.: Vapor pressure and solubility of the aqueous reversible system $2NaCl + MgSO_4 \rightarrow Na_2SO_4 + MgCl_2$. Izvest. Sektora Fiz.-Khim. Anal., Inst. Obsh. Neorg. Khim., Akad. Nauk S.S.S.R. **15**, 234–265 (1947)
200. Reza-Zade, P.F., Rustamov, P.G.: Solubility isotherm of the system $NaCl–MgCl_2–CoSO_4–H_2O$ at 25°. Azerb. Khim. Zhur. (No. 6), 119–125 (1960)
201. Ryspaev, O., Batyrchaev, I.G., Druzhinin, I.G.: Study of the quinary reciprocal system Na^+, Mg^{++}, $Ca^{++} \parallel Cl^-$, $SO_4^{2-}–H_2O$ at 75 °C. Russ. J. Appl. Chem. **48**, 2029–2031 (1975)
202. Susarla, V.R.K.S., Sanghavi, J.R.: Study of the aqueous system Ca^{++}, Na^+, Mg^{++}/Cl^-, SO_4^{2-} at 35 °C. Seventh Symp. Salt **1**, 539–543 (1993)
203. Dinane, A., Mounir, A.: Water activities osmotic and activity coefficients in aqueous mixtures of sodium and magnesium chlorides at 298.15 K by the hygrometric method. Fluid Phase Equilib. **206**, 13–25 (2003)
204. Igelsrud, I., Thompson, T.G.: Equilibria in the saturated solutions of salts occurring in sea water. II. The quaternary system $MgCl_2–CaCl_2–KCl–H_2O$ at 0 °C. J. Am. Chem. Soc. **58**, 318–322 (1936)
205. Assarsson, G.: The winning of salt from the brines in southern Sweden. Sveriges Geol. Undersökn. Ser. C No. 501, Årsbok **42**, 1–15 (1948)
206. Pelling, A.J., Robertson, J.B.: The reciprocal salt-pair: $2NaCl + Ca(NO_3)_2 \rightarrow 2NaNO_3 + CaCl_2$. South Afr. J. Sci. **20**, 236–240 (1923)
207. Lukyanova, E.I., Shoikhet, D.N.: Trudy Gos. Inst. Prikl. Khim. **34**, 10–16 (1940), cited in: Ref. [294], p. 121
208. van Mills, R., Wells, R.C.: Evaporation and concentration of water associated with petroleum and natural gas. Bull. US Geol. Surv. **693**, 1–100 (1919)

209. Pelling, J., Robertson, J.: Chem. J. Met. Min. Soc. South Afr., 196 (1926), cited in: Ref. [165], p. 301
210. Koroleve, V.F.: Trudy Solyanoi Laboratory Akademii Nauk SSSR **15**, 38 (1937), cited in: Ref. [165], p. 303
211. Gromova, E.T.: The solubility isotherm of the Na, Ca ‖ Cl, SO_4–H_2O system at 110 °C. Russ. J. Inorg. Chem. **5**, 1244–1247 (1960)
212. Robinson, R.A., Bower, V.E.: Properties of aqueous mixtures of pure salts. Thermodynamics of the ternary system: water–calcium chloride–magnesium chloride at 25 °C. J. Res. Nat. Bur. Stand. A **70**, 313–318 (1966)
213. Mel'nikova, Z.M., Moshkina, I.A.: The solubility of anhydrite and gypsum in the system Na, Mg, Ca ‖ Cl, SO_4–H_2O at 25 °C. Izv. Akad. Nauk SSSR **4**, 17–25 (1973)
214. Holmes, H.F., Baes Jr., C.F., Mesmer, R.E.: Studies of aqueous solutions at elevated temperatures. III. $\{(1-y)NaCl + (y)CaCl_2\}$. J. Chem. Thermodyn. **13**, 101–113 (1981)
215. Brantley, S.L.: Chapter Two—Activity Coefficients of NaCl–$CaCl_2$ Aqueous Solutions with Application to High Temperature Natural Brines, PhD Thesis, Princeton, pp. 39–62 (1987)
216. Vanko, D.A., Bodnar, R.J., Sterner, S.M.: Synthetic fluid inclusions: VIII. Vapor-saturated halite solubility in part of the system NaCl–$CaCl_2$–H_2O, with application to fluid inclusions from oceanic hydrothermal systems. Geochim. Cosmochim. Acta **52**, 2451–2456 (1988)
217. Lightfoot, W.J., Prutton, C.F.: Equilibria in saturated solutions I. The ternary systems $CaCl_2$–$MgCl_2$–H_2O, $CaCl_2$–KCl–H_2O, and $MgCl_2$–KCl–H_2O at 35 °C. J. Am. Chem. Soc. **68**, 1001–1002 (1946)
218. Lightfoot, W.J., Prutton, C.F.: Equilibria in saturated salt solutions. II. The ternary systems $CaCl_2$–$MgCl_2$–H_2O, $CaCl_2$–KCl–H_2O, and $MgCl_2$–KCl–H_2O at 75 °C. J. Am. Chem. Soc. **69**, 2098–2100 (1947)
219. Lightfoot, W.J., Prutton, C.F.: Equilibria in saturated solutions. III. The quaternary system $CaCl_2$–$MgCl_2$–KCl–H_2O at 35 °C. J. Am. Chem. Soc. **70**, 4112–4115 (1948)
220. Lightfoot, W.J., Prutton, C.F.: Equilibria in saturated salt solutions. IV. The quaternary system $CaCl_2$–$MgCl_2$–KCl–H_2O at 75 °C. J. Am. Chem. Soc. **71**, 1233–1235 (1949)
221. Precht, H., Wittjen, B.: Löslichkeit von Salzgemischen der Salze der Alkalien und alkalischen Erden bei verschiedener Temperatur. Berichte der Deutschen Chemischen Gesellschaft **14**, 1667–1675 (1881)
222. Khaidukov, N.I., Linetzkaya, Z.G.: The water-vapor pressure above the solutions NaCl–KCl–$MgCl_2$–H_2O. Kali **8**, 28–33 (1935)
223. Kistiakovsky, W.: Die wässerigen Lösungen von Doppelsalzen. Z. Physik. Chem. **6**, 97–121 (1890)
224. Feit, W., Kubierschky, K.: Die Gewinnung von Rubidium- und Caesiumverbindungen aus Carnallit. Chemiker Zeitung **16**, 335–340 (1892)
225. Van't Hoff, J.H., Meyerhoffer, W.: Ueber Anwendungen der Gleichgewichtslehre auf die oceanischen Salzablagerungen mit besonderer Berücksichtigung des Stassfurter Salzlagers. Z. Physik. Chem. **30**, 64–88 (1899)
226. Uhlig, J.: The solubility diagram of potassium chloride, magnesium chloride and water at 50°. Centr. Min. Geol., 417–422 (1913)
227. Keitel, H.: The systems KCl–$MgCl_2$–H_2O and NaCl–$MgCl_2$–H_2O. Kali **17**, 248–251, 261–265 (1923)
228. Campbell, A.N., Downs, K.W., Samis, C.S.: The system $MgCl_2$–KCl–$MgSO_4$–K_2SO_4–H_2O at 100 °C. J. Am. Chem. Soc. **56**, 2507–2512 (1934)
229. Lepeshkov, I.N., Bodaleva, N.V.: Solubility isotherm of the aqueous reciprocal system $K_2Cl_2 + MgSO_4 \rightarrow K_2SO_4 + MgCl_2$ at 25°. Izvest. Sekt. Fiz.-Khim. Anal., Inst. Obsh. Neorg. Khim., Akad. Nauk S.S.S.R. **17**, 338–344 (1949)
230. Patel, K.P., Seshadri, K.: Phase rule study of quaternary system potassium chloride–aluminum chloride–magnesium chloride–water at 25°. Ind. J. Chem. **6**, 379–381 (1968)
231. Lee, W.B., Egerton, A.C.: Heterogeneous equilibria between the chlorides of calcium, magnesium, potassium, and their aqueous solutions. Part I. J. Chem. Soc. **123**, 706–716 (1923)
232. Barbaudy, J.: The equilibrium: water-potassium chloride–potassium nitrate–calcium nitrate–calcium chloride. Rec. Trav. Chim. Pays-Bas Belg. **42**, 638–642 (1923)
233. Selivanova, A.S.: Tr. Mosk. Inst. Tonkoi Khim. Tekhnol. **3**, 23 (1952), cited in: Ref. [305], p. 1125
234. Zaslavskii, A.I.: Physicochemical conditions of the crystallization of potassium chlorate at 0° and −10°. Trans. State Inst. Appl. Chem. (U.S.S.R.) No. 23, 67–84 (1935)
235. Assarsson, G.O.: Equilibria in aqueous systems containing K^+, Na^+, Ca^{++}, Mg^{++} and Cl^-. I. The ternary system $CaCl_2$–KCl–H_2O. J. Am. Chem. Soc. **72**, 1433–1436 (1950)
236. Vlasov, N.A., Ogienko, S.V.: Solubility polytherms of the system $CaCl_2$–KCl–H_2O from the temperature of complete freezing to +40°. Izv. Fiz.-Khim. Nauchn.-Issled. Inst. Pri Irkutskom Univ. **4**, 62–80 (1959)
237. Kolesnikov, M.M., Beskov, S.D., Druzhinin, I.G.: Uchenyie Zapiski **193**, 47 (1968), cited in: Ref. [165], p. 675

238. Soloveva, E.F.: The 50° isotherm of the aqueous salt system Na^+, K^+, Mg^{2+}, $Ca^{2+}//Cl^-$–H_2O. Tr. Vses. Nauch.-Issled. Inst. Geologii No. 52, 58–74 (1967)
239. Kurnakov, N.S., Nikolaev, A.V.: Izv. Akad. Nauk SSSR Ser. Khim. **2**, 403–313 (1938)
240. Smith, A., Prutton, C.: Patent 1768797, U.S.A. (1923)
241. Smith, A., Prutton, C.: Patent 1780098, U.S.A. (1923)
242. Bury, C.R., Davies, E.R.H.: The system magnesium chloride–lime–water. J. Chem. Soc., 701–705 (1933)
243. Yanatieva, O.K.: Polytherms of solubility of salts in the tropic systems $CaCl_2$–$MgCl_2$–H_2O and $CaCl_2$–NaCl–H_2O. Russ. J. Appl. Chem. **19**, 709–722 (1946)
244. Assarsson, G.O.: Equilibria in aqueous systems containing K^+, Na^+, Ca^{2+}, Mg^{2+}, and Cl^-. III. The ternary system $CaCl_2$–$MgCl_2$–H_2O. J. Am. Chem. Soc. **72**, 1442–1444 (1950)
245. Perova, A.P.: Mutual solubility of the ternary system $CaCl_2$–$MgCl_2$–H_2O at 55°. Soobsh. Nauch. Rabot Vsesoyuz. Khim. Obsh. im. D.I. Mendeleeva (No. 2), 46–48 (1955)
246. Uyeda, K.: On the equilibrium of the reciprocal salt pair: $ClK + NO_3K + ClNa$. Memoirs Coll. Sci. Eng. Kyoto Imp. University **2**, 245–261 (1910)
247. Leather, J.W., Mukerji, J.N.: The system potassium nitrate, sodium chloride, water. Mem. Dept. Agr. India, Chem. Ser. **3**, 177–204 (1913)
248. Nichol, W.W.J.: On the mutual solubility of salts in water. Part I. Philos. Mag. J. Sci. **31**, 369–385 (1891)
249. Benrath, A.Z.: Über die Löslichkeit von Salzen und Salzgemischen bei Temperaturen oberhalb von 100 °C. Z. Anorg. Chem. **252**, 86–94 (1943)
250. Cornec, E., Krombach, H.: The study of equilibria between water the nitrates, chlorides and sulfates of sodium and potassium. Ann. Chim. Appl. **12**, 203–295 (1929)
251. Carnelley, T., Thomson, A.: The solubility of isomeric organic compounds and of mixtures of sodium and potassium nitrates, and the relation of solubility to fusibility. J. Chem. Soc. **53**, 782–802 (1888)
252. Kremann, R., Zitek, A.: Die Bildung von Konversionssalpeter aus Natronsalpeter und Pottasche vom Standpunkt der Phasenlehre. Monatsh. Chem. **30**, 311–340 (1909)
253. Madgin, W.M., Briscoe, H.V.A.: The melting-point (solidus) curve for mixtures of potassium nitrate and sodium nitrate. J. Chem. Soc. **123**, 2914–2916 (1923)
254. Hamid, M.A.: Heterogeneous equilibria between the sulphates and nitrates of sodium and potassium and their aqueous solution. Part I. The ternary systems. J. Chem. Soc., 199–205 (1926)
255. Nikolaev, V.I.: Partition of nitric acid between sodium and potassium hydroxide. J. Russ. Phys. Chem. Soc. **60**, 893–904 (1928)
256. Ravich, M.I., Ginzburg, F.B.: State diagram of the ternary system KNO_3–$NaNO_3$–H_2O. Bull. Acad. Sci. U.R.S.S. Classe Sci. Chim. (No. 2), 141–151 (1947)
257. Karnaukhov, A.S., Uch. Zap. Yaroslav. Gos. Pedagog. Inst. **31**, 255 (1956), cited in: Ref. [305], p. 768
258. Jackman, D.N., Browne, A.: The 25 °C-isotherms of the systems magnesium nitrate–sodium nitrate–water and magnesium sulphate–magnesium nitrate–water. J. Chem. Soc. **121**, 694–697 (1922)
259. Benrath, A.: Study of $MgSO_4$–$NaNO_3$–H_2O. I. Caliche **11**, 99–126 (1929)
260. Schroder, W.: Über das reziproke Salzpaar $MgSO_4$–$Na_2(NO_3)_2$–H_2O. V. Z. Anorg. Allgem. Chem. **185**, 153–166 (1929)
261. Schroder, W.: Über das reziproke Salzpaar $MgSO_4$–$Na_2(NO_3)_2$–H_2O. VI. Z. Anorg. Allgem. Chem. **185**, 267–279 (1929)
262. Sieverts, A., Muller, H.: The reciprocal salt pair $MgCl_2$, $Na_2(NO_3)_2$, H_2O. I. Z. Anorg. Allgem. Chem. **189**, 241–57 (1930)
263. Hamid, M.A., Das, R.: The system: water–potassium nitrate–calcium nitrate. J. Indian Chem. Soc. **7**, 881–882 (1930)
264. Frowein, F.: Das System $K_2/Ca/Na_2/(NO_3)_2/H_2O$. Z. Anorg. Allgem. Chem. **169**, 336–344 (1928)
265. Kremann, R., Rodemund, H.: Über das Auftreten eines Tripelsalzes aus wässerigen Lösungen ohne gleichzeitiger Bildung eines binären Doppelsalzes. Z. Anorg. Chem. **86**, 373–379 (1914)
266. Benrath, A., Sichelschmidt, A.: Das reziproke Salzpaar $MgSO_4 + K_2(NO_3)_2 \rightarrow Mg(NO_3)_2 + K_2SO_4$. III. Z. Anorg. Allgem. Chem. **197**, 113–128 (1931)
267. Bergman, A.G., Opredelenkova, L.V.: Solubility polytherms of the calcium nitrate–potassium nitrate–water and calcium nitrate–potassium chloride–water ternary systems. Russ. J. Inorg. Chem. **14**, 1144–1146 (1969)
268. Hamid, M.A., Das, R.: The system: water–potassium nitrate–calcium nitrate. J. Indian Chem. Soc. **7**, 881–882 (1930)
269. Yakimov, M.A., Guzhavina, E.I., Lazeeva, M.S.: Solution–vapour equilibrium in calcium (cadmium) nitrate–alkali metal nitrate–water systems. Russ. J. Inorg. Chem. **14**, 1011–1014 (1969)
270. Goloshchapov, M.V.: Reciprocal solubility in the system $Ca(NO_3)_2$–$Mg(NO_3)_2$–H_2O. Izv. Voronezh. Gosudarst. Pedagog. Inst. **16**, 19–31 (1955)

271. Frolov, A.A., Orlova, V.T., Lepeshkov, I.N.: Solubility polytherm of the system $Ca(NO_3)_2$–$Mg(NO_3)_2$–H_2O. Inorg. Mater. **28**, 1040–1042 (1992)
272. Nikolaev, V.I.: The distribution of strong bases and strong acids in saturated water solutions. Z. Anorg. Allgem. Chem. **181**, 249–79 (1929)
273. Reinders, W.: Die reziproken Salzpaare $KCl + NaNO_3 = KNO_3 + NaCl$ und die Bereitung von Konversionssalpeter. Z. Anorg. Allgem. Chem. **93**, 202–212 (1915)
274. Rüdorff, F.: Über die Löslichkeit von Salzgemischen. Ber. Deutsc. Chem. Gesellschaft **6**, 482–486 (1873)
275. Wurmser, M.: Preparation of ammonium nitrate. Compt. Rend. **174**, 1466–1468 (1922)
276. Cornec, E., Chretion, A.: The system sodium nitrate, sodium chloride and water. Caliche **6**, 358–369 (1924)
277. Findlay, A., Cruickshank, J.: The reciprocal salt pair (Na, Ba)–(Cl, NO_3) in aqueous solution at 20 °C. J. Chem. Soc., 316–318 (1926)
278. Sheludko, M.K., Kulish, N.F.: Tr. Dnepropetrovsk. Khimii Tekhnol. Inst. Vyp. **5**, 201 (1956), cited in: Ref. [305], p. 175
279. Bursa, S., Kitowska, M.: Liquid–solid equilibrium in the $NaNO_3$–NaCl–HNO_3–HCl–H_2O system. Przemysl Chem. **47**, 103–106 (1968)
280. Straszko, J., Kowalczyk, R.: Liquid–solid equilibrium in the $NaNO_3$–NaCl–HNO_3–HCl–H_2O system. Przemysl Chem. **53**, 97–99 (1976)
281. Soch, C.A.: Fractional crystallization. J. Phys. Chem. **2**, 43–50 (1898)
282. Kritschewski, I., Izkowitsch, R.K.: Das reziproke Salzpaar $Ca(NO_3)_2 + 2KCl \rightarrow 2KNO_3 + CaCl_2$ bei −10 °C. Z. Anorg. Allgem. Chem. **215**, 103–104 (1933)
283. Bodlaender, G.: Über die Löslichkeit einiger Stoffe in Gemischen von Wasser und Alkohol. Z. Physik. Chem. **7**, 308–322 (1891). Über die Löslichkeit von Salzgemischen in Wasser. Z. Physik. Chem. **7**, 358–366 (1891)
284. Touren, C.: Solubility of a mixture of salts having a common ion. Compt. Rendus Hebd. Seances Acad. Sci. **131**, 259 (1900)
285. Armstrong, H.E., Eyre, J.V.: Studies in the processes operative in solutions. XI. The displacement of salts from solution by various precipitants. Proc. Roy. Soc. London (A) **84**, 123–135 (1911)
286. Tanaka, H.: Preparation of potassium nitrate and alumina by double decomposition of potassium chloride and aluminum nitrate. I. The system $3KCl + Al(NO_3)_3 \rightarrow 3KNO_3 + AlCl_3$. Kogyo Kagaku Zasshi **33**, 488–492 (1930)
287. Benrath, A., Braun, A.: Über die Löslichkeit von Salzen und Salzgemischen in Wasser bei Temperaturen oberhalb von 100 °C. II. Z. Anorg. Allgem. Chem. **244**, 348–358 (1940)
288. Zhang, L., Gui, Q., Lu, X., Wang, Y., Shi, J., Lu, B.C.-Y.: Measurement of solid-liquid equilibria by a flow-cloud-point method. J. Chem. Eng. Data **43**, 32–37 (1998)
289. Ehret, W.F.: Ternary systems $CaCl_2$–$Ca(NO_3)_2$–H_2O (25 °C), $CaCl_2$–$Ca(ClO_3)_2$–H_2O (25 °C), $SrCl_2$–$Sr(NO_3)_2$–H_2O (25 °C), KNO_3–$Pb(NO_3)_2$–H_2O (0 °C). J. Am. Chem. Soc. **54**, 3126–3134 (1932)
290. Matsuo, T., Takeda, A.: Studies on brine obtained by the ion exchange membrane method. II. Crystallizing areas of potassium chloride, carnalite, and other salts in equilibrium system of brine produced by ion exchange membrane method. Nippon Kaisui Gakkaishi **25**, 129–141 (1971)
291. d'Ans, J., Bertsch, A., Gessner, A.: Untersuchungen über Salzsysteme ozeanischer Salzablagerungen. Kali **9**, 148–154 (1915)
292. Kayser, E.: Substitution factors for dissimilarly saturated solutions of potassium chloride and sodium chloride. Kali **17**, 1–9, 37–42 (1923)
293. Serowy: Die Polythermen der Viersalzpunkte des Chlorkaliumfeldes im quinären System ozeanischer Salzblagerungen; ihre teilweise Nachprüfung und Vervollständigung bis zu Temperaturen über 100°. Kali **17**, 345–350 (1923)
294. Pelsha, A.D.: Handbook of Experimental Data of Salt Solubilities, Quaternary and More Complex Systems, vol. 2. Khimia, Leningrad (1975)
295. Ilinskii, V.P., Varypaev, N.A., Gitterman, K.E., Shmidt, N.E.: Trudy Solyanoi Laboratory Akademii Nauk SSSR **7**, 10 (1936), cited in Ref. [165], p. 302
296. Van't Hoff, J.H.: Zur Bildung der ozeanischen Salzablagerungen. Sitzungsber. Preuss. Acad. Wissen., Lichtenstein, pp. 232–235 (1905)
297. Igelsrud, I., Thompson, T.G.: Equilibria in the saturated solutions of salts occurring in sea water. II. The quaternary system $MgCl_2$–$CaCl_2$–KCl–H_2O at 0 °C. J. Am. Chem. Soc. **58**, 2003–2009 (1936)
298. Assarsson, G.O., Balder, A.: The poly-component aqueous systems containing the chlorides of Ca^{++}, Mg^{++}, Sr^{++}, K^+ and Na^+ between 18 and 93 °C. J. Phys. Chem. **59**, 631–633 (1955)
299. Khitrova, N.N.: Physicochemical investigation of a four-component reciprocal aqueous solution of sodium and potassium chlorides and nitrates. Izvest. Sekt. Fiz. Khim. Anal., Inst. Obsh. Neorg. Khim., Akad. Nauk S.S.S.R. **27**, 344–357 (1956)

300. Etard, M.: Recherches expérimentales sur les solutions saturées. Ann. Chim. Phys. **3**, 275–288 (1894)
301. Karsten: Ann. der Chem. U. Pharm. Suppl. **3**, 170 (1865), cited in Ref. [305], p. 1124
302. Ritzel, A.: Die Krystalltracht des Chlornatriums in ihrer Abhängigkeit vom Lösungmittel. Z. Kristallographie Mineral **49**, 152–192 (1911)
303. Babenko, A.M.: Study of solubility in the system Na^+, $K^+ \| Cl^-$, NO_3^-–H_2O. Russ. J. Appl. Chem. **48**, 1820–1824 (1975)
304. Bergman, A.G., Nagornyi, G.I.: Polytherm of the reciprocal system of magnesium and potassium chlorides and nitrates (the conversion of magnesium nitrate). Bull. Acad. Sci. U.R.S.S., Classe Sci. Math. Nat., Ser. Chim. No. 1, 217–228 (1938)
305. Silcock, H.L.: Solubilities of Inorganic and Organic Compounds, Ternary and Multicomponent Systems of Inorganic Substances, vol. 3, Part 2. Pergamon, Oxford (1979)